Lecture 6:

Evidence of evolution:
Homologies

Course 410

Molecular Evolution

ho·mol·o·gous | hōˈmäləgəs |

adjective

having the same relation, relative position, or structure.

- *Biology* (of organs) similar in position, structure, and evolutionary origin but not necessarily in function: *a seal's flipper is* ***homologous with*** *the human arm*. Often contrasted with analogous.
- *Biology* (of chromosomes) pairing at meiosis and having the same structural features and pattern of genes.
- *Chemistry* (of a series of chemical compounds) having the same functional group but differing in composition by a fixed group of atoms.

ORIGIN

mid 17th century: via medieval Latin from Greek ***homologos*** 'agreeing, consistent', from ***homos*** 'same' + ***logos*** 'ratio, proportion'.

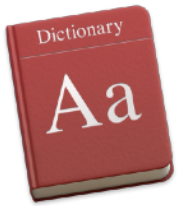

Cellular homology

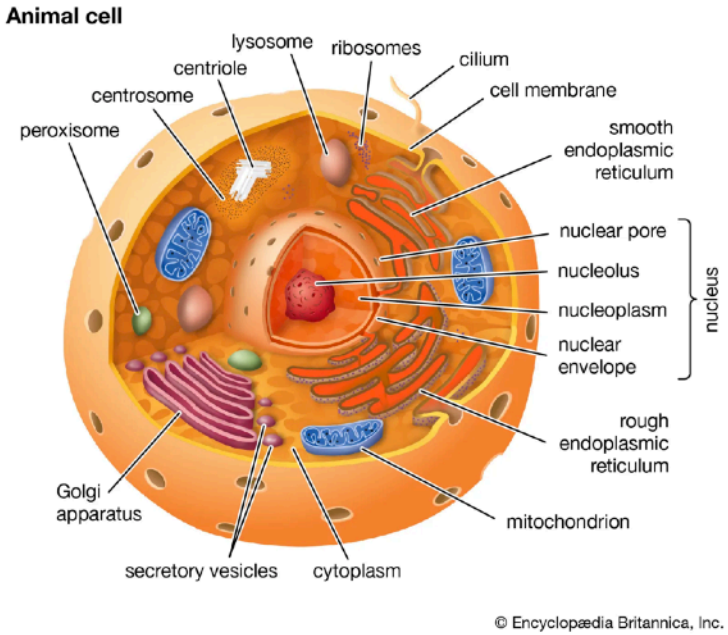
Animal cell
lysosome
ribosomes
cilium
centriole
centrosome
cell membrane
peroxisome
smooth endoplasmic reticulum
nuclear pore
nucleolus
nucleoplasm
nuclear envelope
nucleus
rough endoplasmic reticulum
Golgi apparatus
mitochondrion
secretory vesicles
cytoplasm
© Encyclopædia Britannica, Inc.

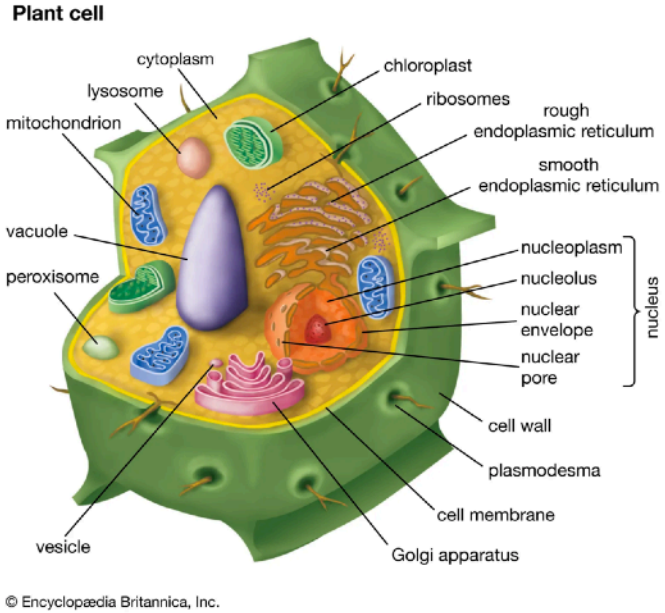
Plant cell
cytoplasm
chloroplast
lysosome
ribosomes
rough endoplasmic reticulum
mitochondrion
smooth endoplasmic reticulum
vacuole
nucleoplasm
peroxisome
nucleolus
nuclear envelope
nuclear pore
nucleus
cell wall
plasmodesma
cell membrane
vesicle
Golgi apparatus
© Encyclopædia Britannica, Inc.

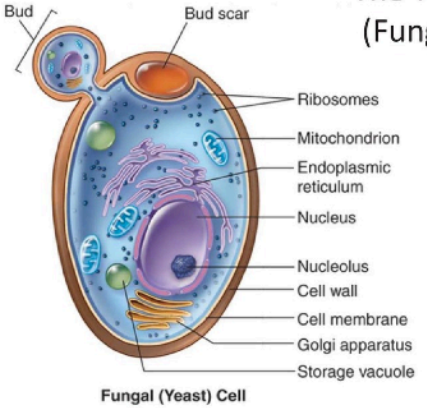
The Yeast Cell
(Fungal Cell)
Bud
Bud scar
Ribosomes
Mitochondrion
Endoplasmic reticulum
Nucleus
Nucleolus
Cell wall
Cell membrane
Golgi apparatus
Storage vacuole
Fungal (Yeast) Cell

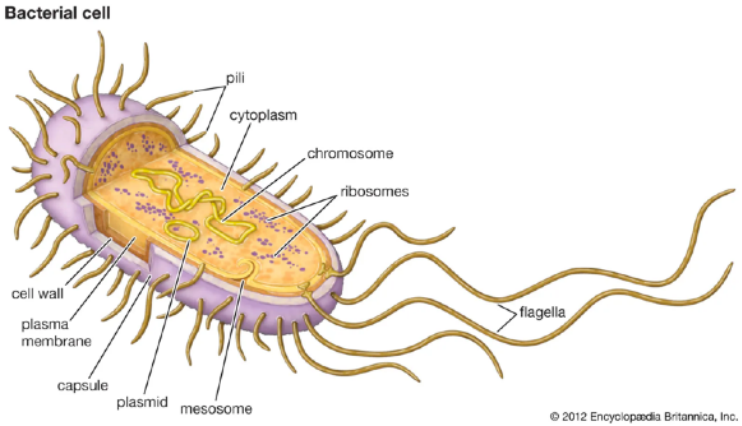
Bacterial cell
pili
cytoplasm
chromosome
ribosomes
cell wall
plasma membrane
flagella
capsule
plasmid
mesosome
© 2012 Encyclopædia Britannica, Inc.

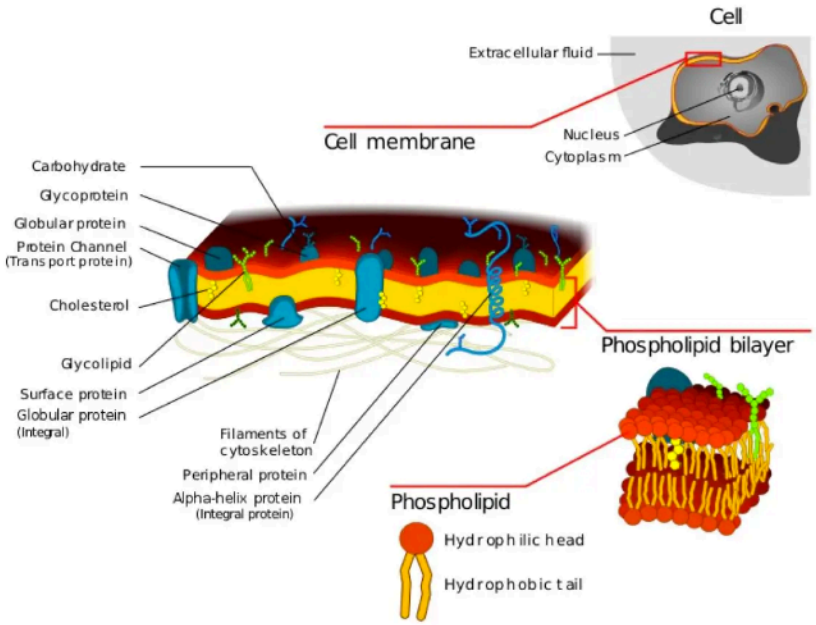
Cell
Extracellular fluid
Cell membrane
Nucleus
Cytoplasm
Carbohydrate
Glycoprotein
Globular protein
Protein Channel
(Transport protein)
Cholesterol
Glycolipid
Surface protein
Globular protein
(Integral)
Filaments of
cytoskeleton
Peripheral protein
Alpha-helix protein
(Integral protein)
Phospholipid bilayer
Phospholipid
Hydrophilic head
Hydrophobic tail

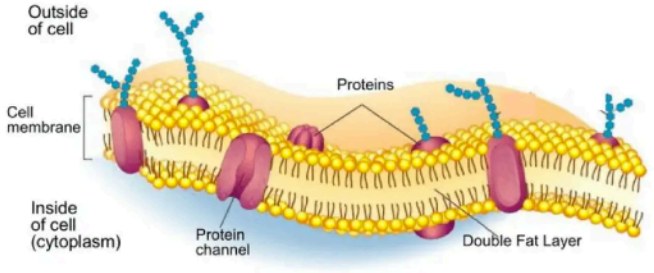
Outside
of cell
Proteins
Cell
membrane
Inside
of cell
(cytoplasm)
Protein
channel
Double Fat Layer

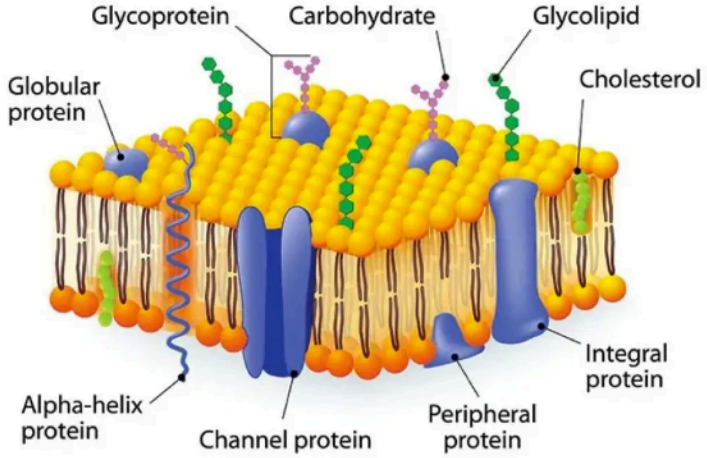
Glycoprotein
Carbohydrate
Glycolipid
Globular
protein
Cholesterol
Integral
protein
Alpha-helix
protein
Channel protein
Peripheral
protein

Primer

Membranes and evolution

Sven B. Gould

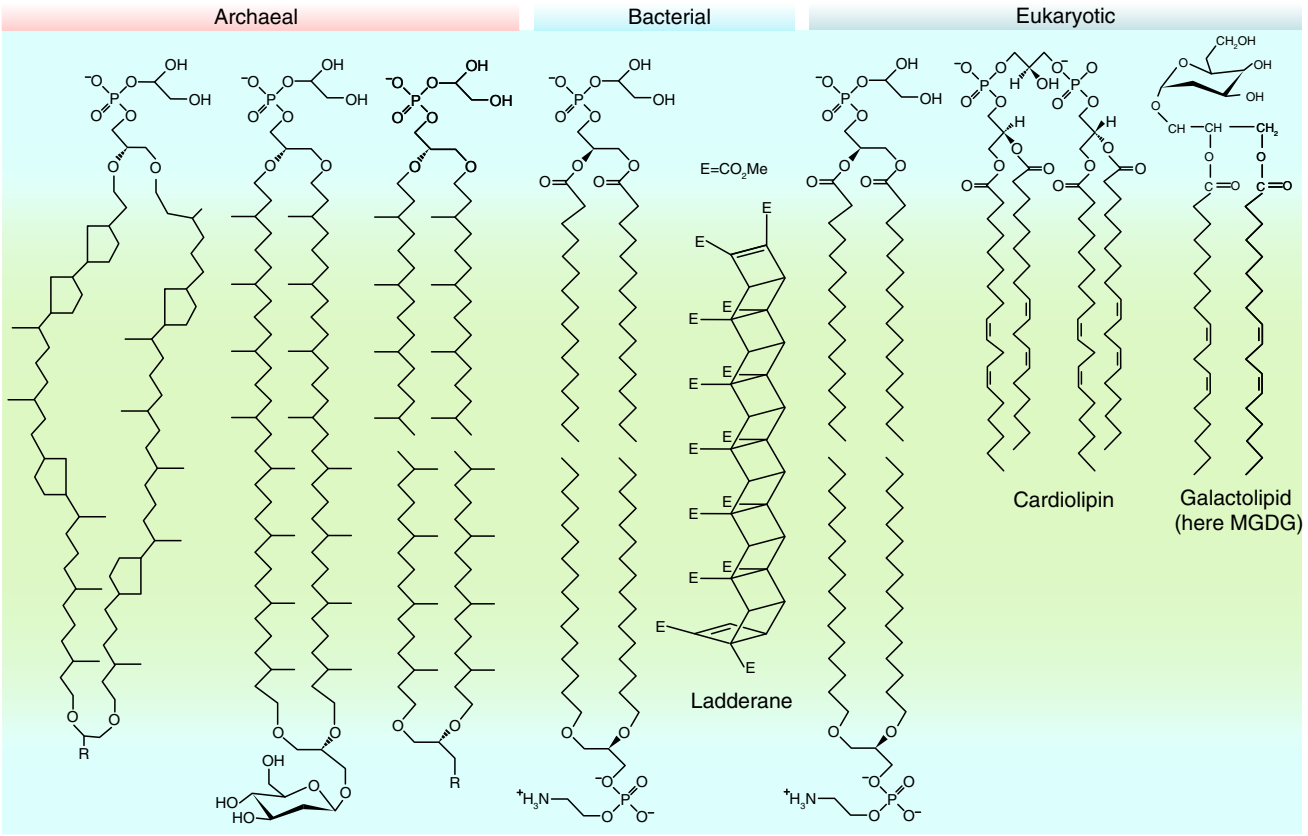

Figure 2. Exemplary lipid species.
Many hundred different types of lipids have been characterized, but some generalizations can be made. Archaea contain a variety of lipids that are characterized by isoprenoid chains, which are ether-linked to the hydrophilic head group and can span an entire membrane, thereby generating a mono- instead of a more canonical bilayer. They are generally less permeable and the plasma membranes they constitute are often covered with a paracrystalline protein layer, the S-layer. Bacterial lipids are characterized by glycerol-3-phosphates linked to fatty acid side chains through an ester bond. Membranes can be enriched with molecules other than proteins, such as the bacterial ladderane that makes a membrane less permeable. The main lipid types of eukaryotes are like those of bacteria and none of their many compartments share an identical lipid composition. The two compartments of endosymbiotic origin, the mitochondrion and plastid, are characterized by their very own specific lipid types, cardiolipin and galactolipids, respectively. Both of these lipid types play a role in stabilizing components of the organelle's different electron transport chains and are lost in organelles that no longer synthesize ATP through chemiosmotic coupling.

Endosymbiosis

en·do·sym·bi·o·sis | ˌendōˌsimbīˈōsəs |

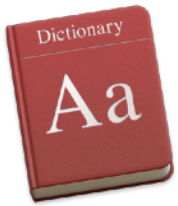

noun *Biology*

symbiosis in which one of the symbiotic organisms lives inside the other.

Aerobic proteobacterium

Cyanobacterium

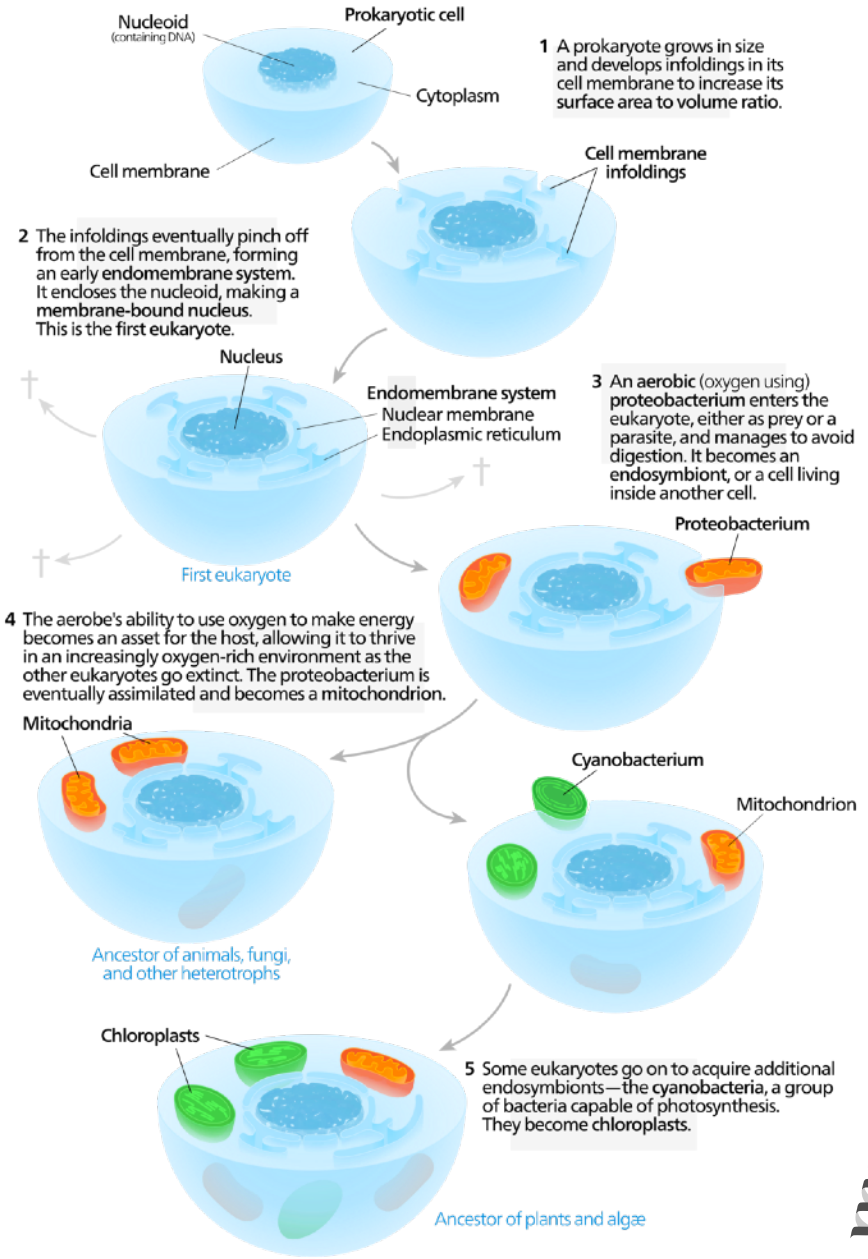

Mitochondrial genome

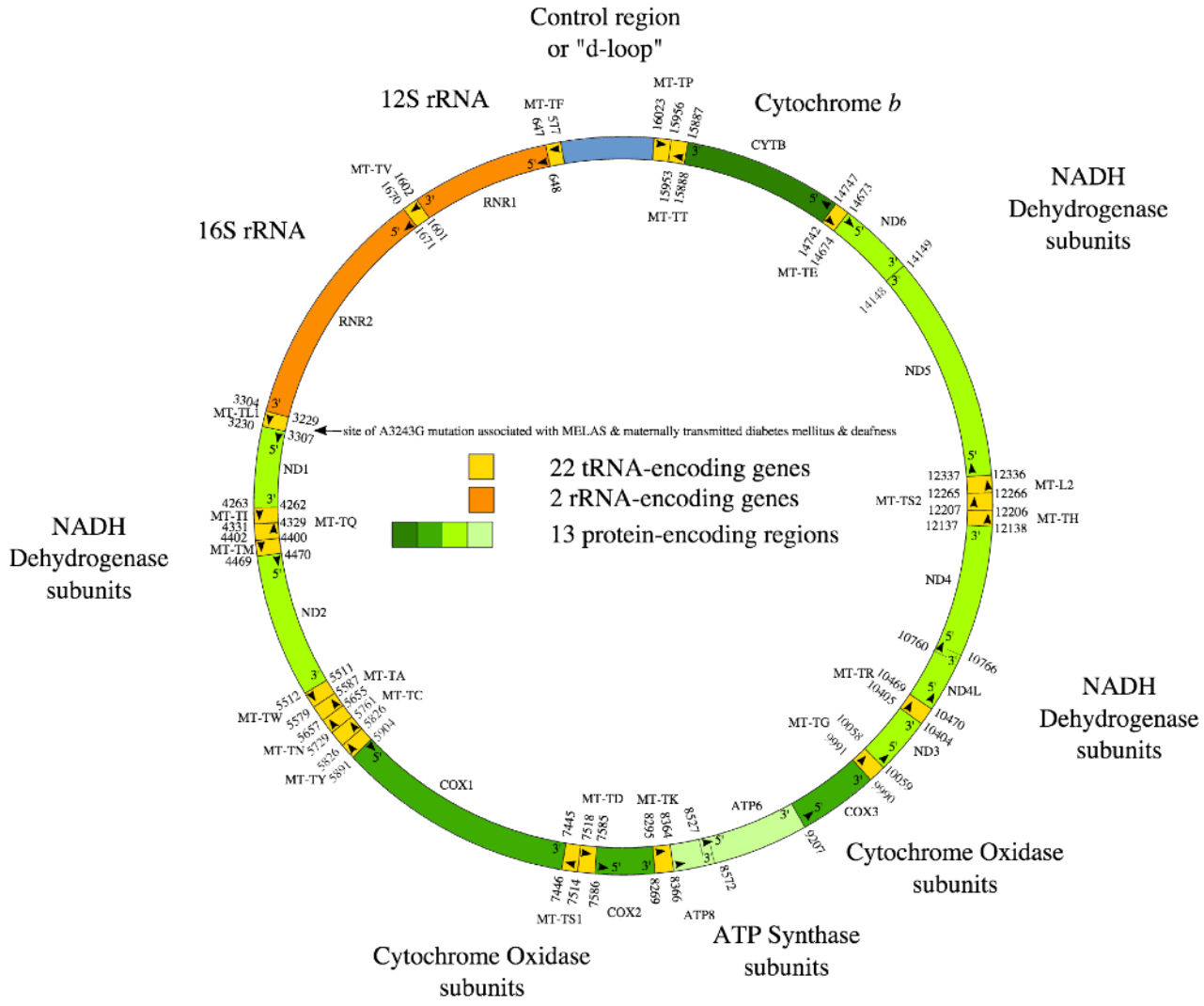
Control region
or "d-loop"
12S rRNA
Cytochrome b
16S rRNA
NADH
Dehydrogenase
subunits
NADH
Dehydrogenase
subunits
NADH
Dehydrogenase
subunits
Cytochrome Oxidase
subunits
ATP Synthase
subunits
Cytochrome Oxidase
subunits
MT-TP
MT-TF
MT-TV
MT-TT
MT-TE
CYTB
RNR1
RNR2
ND6
ND5
ND4
ND4L
ND3
COX3
ATP6
ATP8
COX2
MT-TS1
COX1
MT-TD
MT-TK
MT-TG
MT-TR
MT-TH
MT-L2
MT-TS2
MT-TQ
MT-TI
MT-TM
ND2
MT-TA
MT-TC
MT-TW
MT-TN
MT-TY
ND1
MT-TL1
site of A3243G mutation associated with MELAS & maternally transmitted diabetes mellitus & deafness
22 tRNA-encoding genes
2 rRNA-encoding genes
13 protein-encoding regions

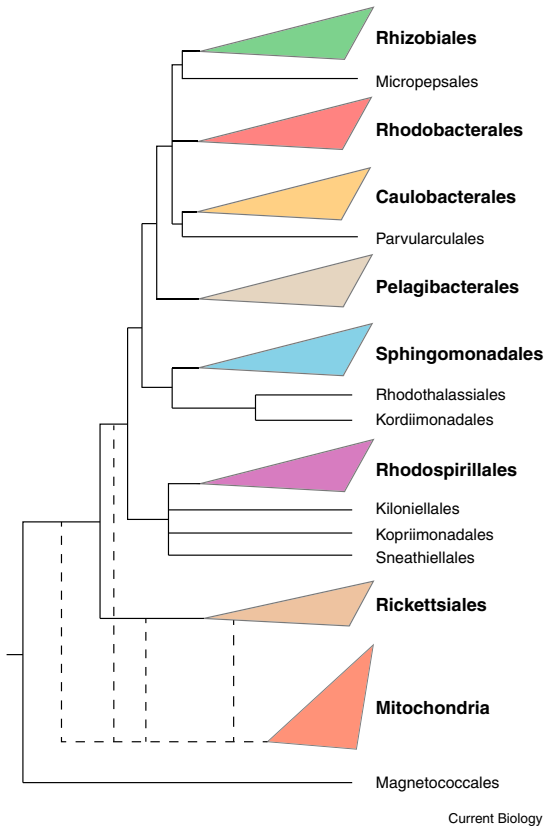

Figure 2. The phylogenetic position of mitochondria among alphaproteobacteria remains contentious.
The class Alphaproteobacteria encompasses well-defined diverse orders: the Rhizobiales, Rhodobacterales, Caulobacterales, Sphingomonadales, Pelagibacterales (SAR11), Rhodospirillales, and Rickettsiales [5,35] (the order Magnetococcales [36] is a distant sister to all other alphaproteobacteria). Some recently proposed candidate orders with sole or few representatives are also depicted (see [129]). The mitochondrial lineage could be placed at the base of Alphaproteobacteria, as sister to all 'free-living' alphaprotebacteria (e.g., [14]) as sister to the Rickettsiales or within the Rickettsiales (e.g., [13]); all positions are shown with dashed lines. Alphaproteobacteria are incredibly diverse. The Rhizobiales include plant-associated nitrogen-fixing rhizobia, facultative intracellular parasites as well as methanotrophs. The order Rhodobacterales encompasses purple non-sulfur bacteria, as well as abundant aerobic oceanic phototrophs and diverse heterotrophs. Some of the most abundant bacteria in the ocean are the small heterotrophic pelagibacterales. The Rickettsiales is composed exclusively of obligately intracellular endosymbionts or parasites. Phototrophs are found among the Rhizobiales, Rhodobacterales, Caulobacterales, Sphingomonadales, and Rhodospirillales.

The Origin and Diversification of Mitochondria

Andrew J. Roger[1,*], Sergio A. Muñoz-Gómez[1], and Ryoma Kamikawa[2]

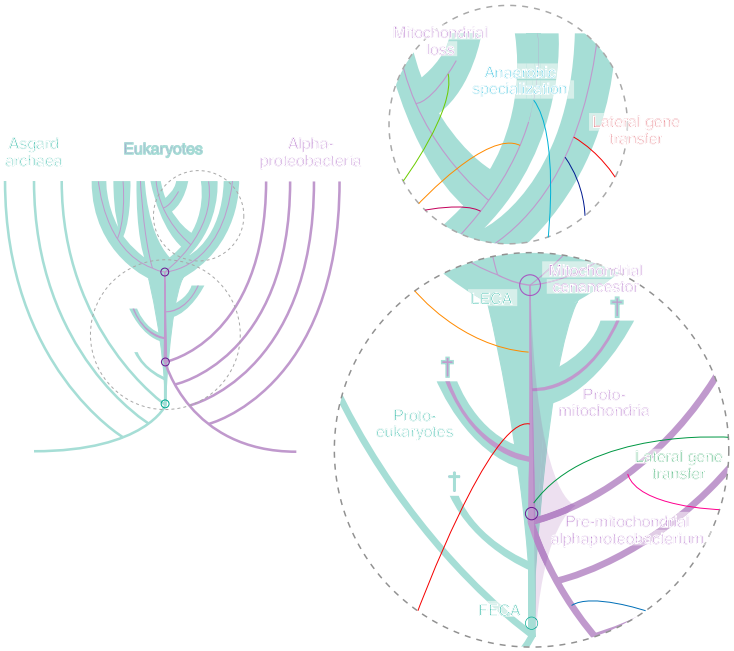

Figure 1. The origin and evolution of mitochondria and eukaryotes.
Mitochondria evolved from an endosymbiotic alphaproteobacterium (purple) within an archaeal-derived host cell that was most closely related to Asgard archaea (green). The earliest ancestor of mitochondria (that is not also an ancestor of an extant alphaproteobacterium) is the pre-mitochondrial alphaproteobacterium. Proto-mitochondria evolved from this first alphaproteobacterial endosymbiont, and comprise all transitional forms of mitochondria before the mitochondrial cen-ancestor, the mitochondrion in the last eukaryotic common ancestor (LECA). The timing of the mitochondrial endosymbiosis is uncertain (indicated by a purple shadow along the proto-eukaryotic stem) but postdates the first eukaryote common ancestor (FECA) and predates LECA. As far as we know, transitional 'proto-eukaryotes' between FECA and LECA went extinct (indicated by crosses). The complexity of the proto-eukaryotic genome and proteome gradually increased during eukaryogenesis (increasingly wider green branches), but the mitochondrial endosymbiont's genome and proteome were reduced, as the organelle incorporated proteins of host and foreign origin (progressively thinner purple branches for the mitochondrial endosymbiont contribution, with thin coloured branches indicating lateral gene transfers). Adaptations of mitochondria to anaerobiosis and outright loss of mitochondria (upper right circle) were facilitated by lateral gene transfer events.

Chloroplast genome

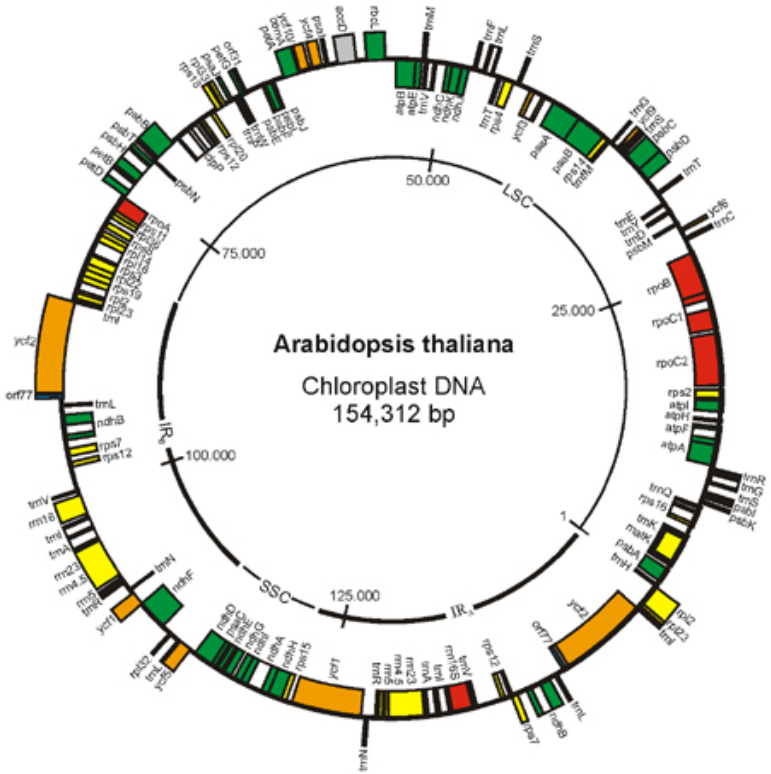

A. thaliana chloroplast DNA (inner circle: clockwise, outer: counter-clockwise). Function: transcription (red), translation (yellow), photosynthesis (green), tRNA (black), other (gray), unknown (orange). Sequence: AP000423 (see Sato et al., DNA Res 6: 283-290, 1999).

An Expanded Ribosomal Phylogeny of Cyanobacteria Supports a Deep Placement of Plastids

Kelsey R. Moore[1], Cara Magnabosco[2], Lily Momper[1], David A. Gold[3], Tanja Bosak[1] and Gregory P. Fournier[1]*

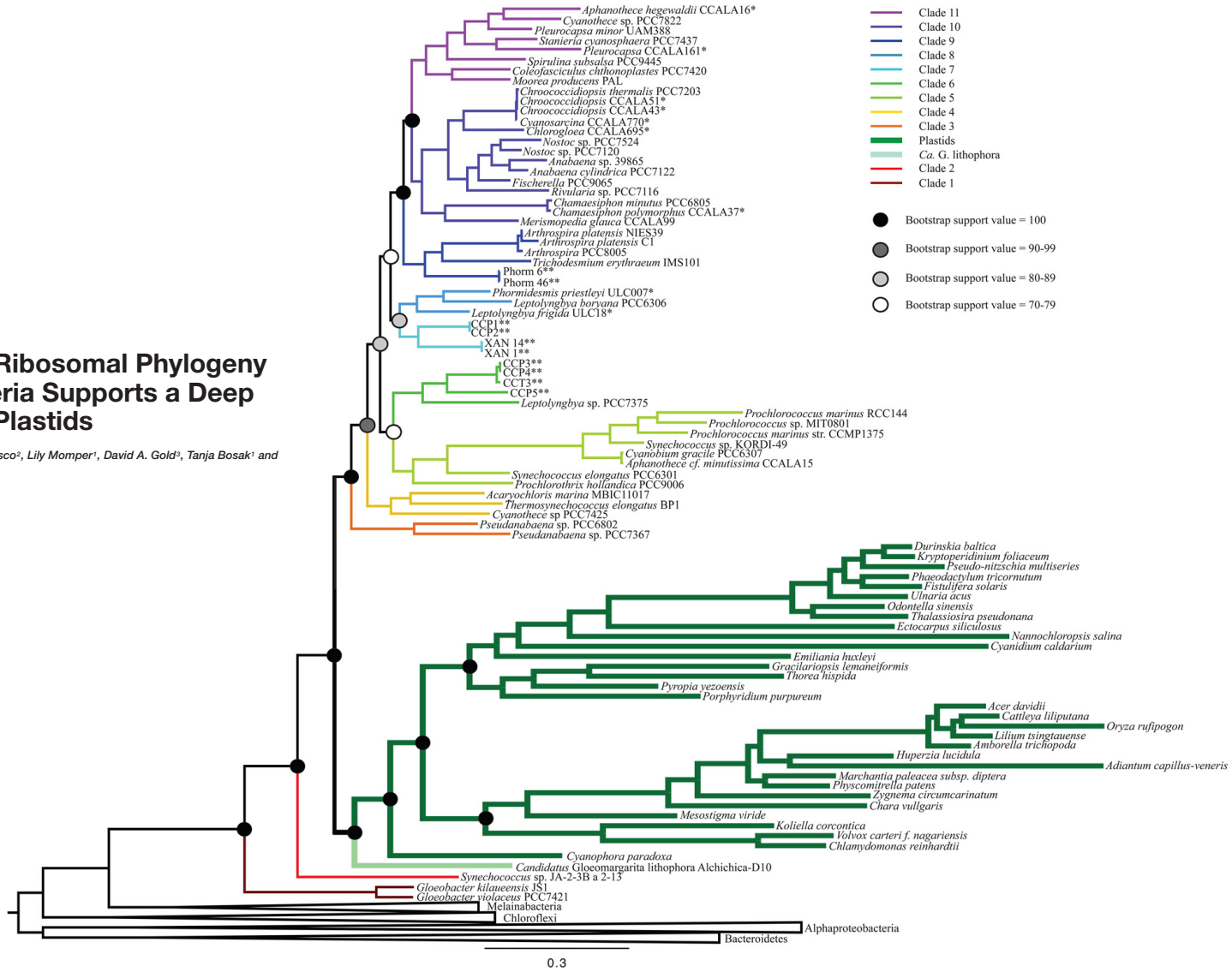

FIGURE 1 | A maximum likelihood (ML) phylogenetic tree made using a concatenation of 30 large and small subunit ribosomal proteins (**Table 2**) and RAxML. This tree supports a deep placement of the plastid clade with high bootstrap support. Bootstrap values are denoted for major divergences of cyanobacterial and plastid clades. All internal nodes have bootstrap values of >90.

Organ homology

human

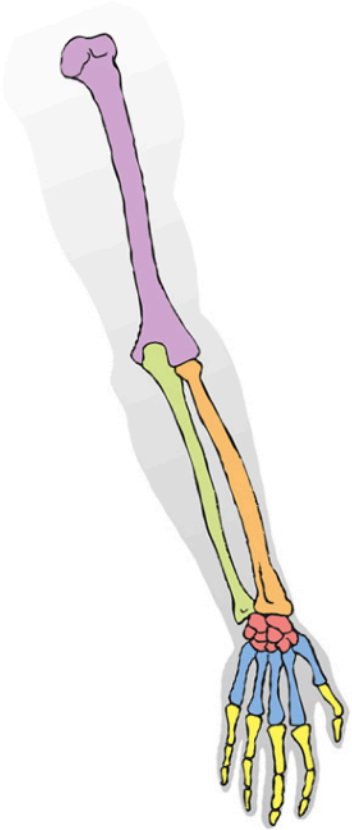

horse

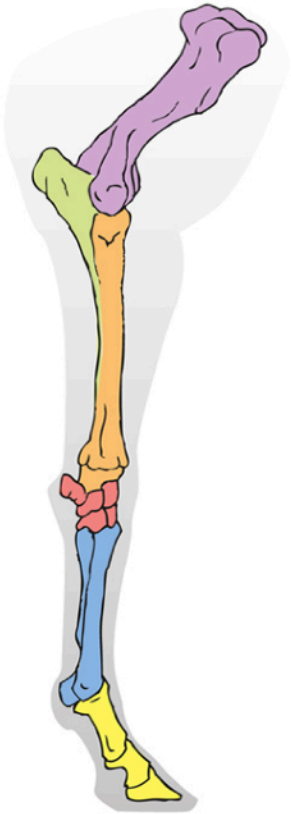

dolphin

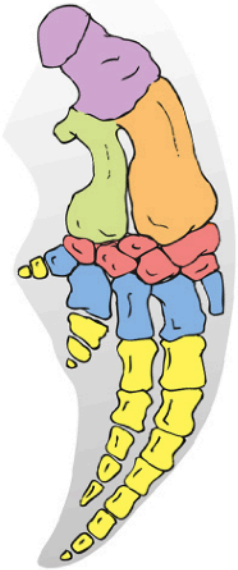

bat

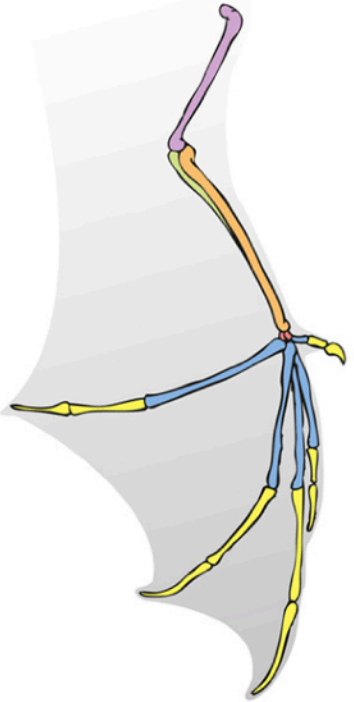

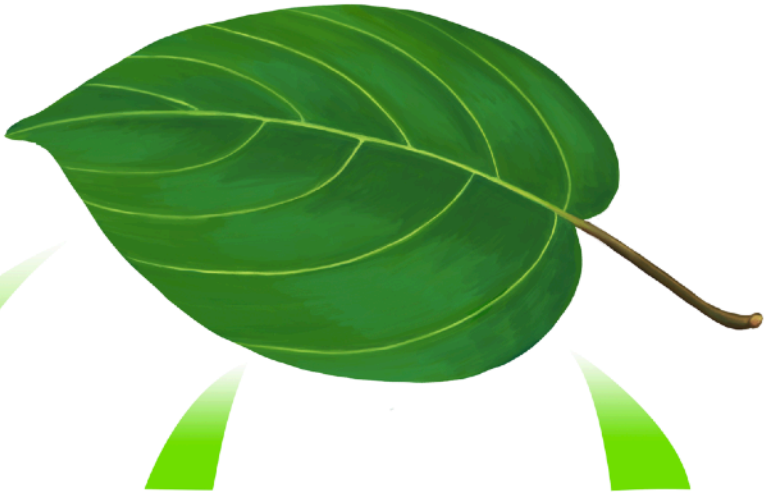

pitcher plant
leaves modified into pitchers to catch insects

Venus flytrap
leaves modified into jaws to catch insects

poinsettia
bright red leaves resemble flower petals

cactus
leaves have become spines

Homologous vs. analogous

a·nal·o·gous | əˈnaləgəs |

adjective (often **analogous to**)

comparable in certain respects, typically in a way which makes clearer the nature of the things compared: *they saw the relationship between a ruler and his subjects as* ***analogous to*** *that of father and children.*

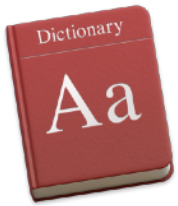

• *Biology* (of structures) performing a similar function but having a different evolutionary origin, such as the wings of insects and birds. Often contrasted with homologous.

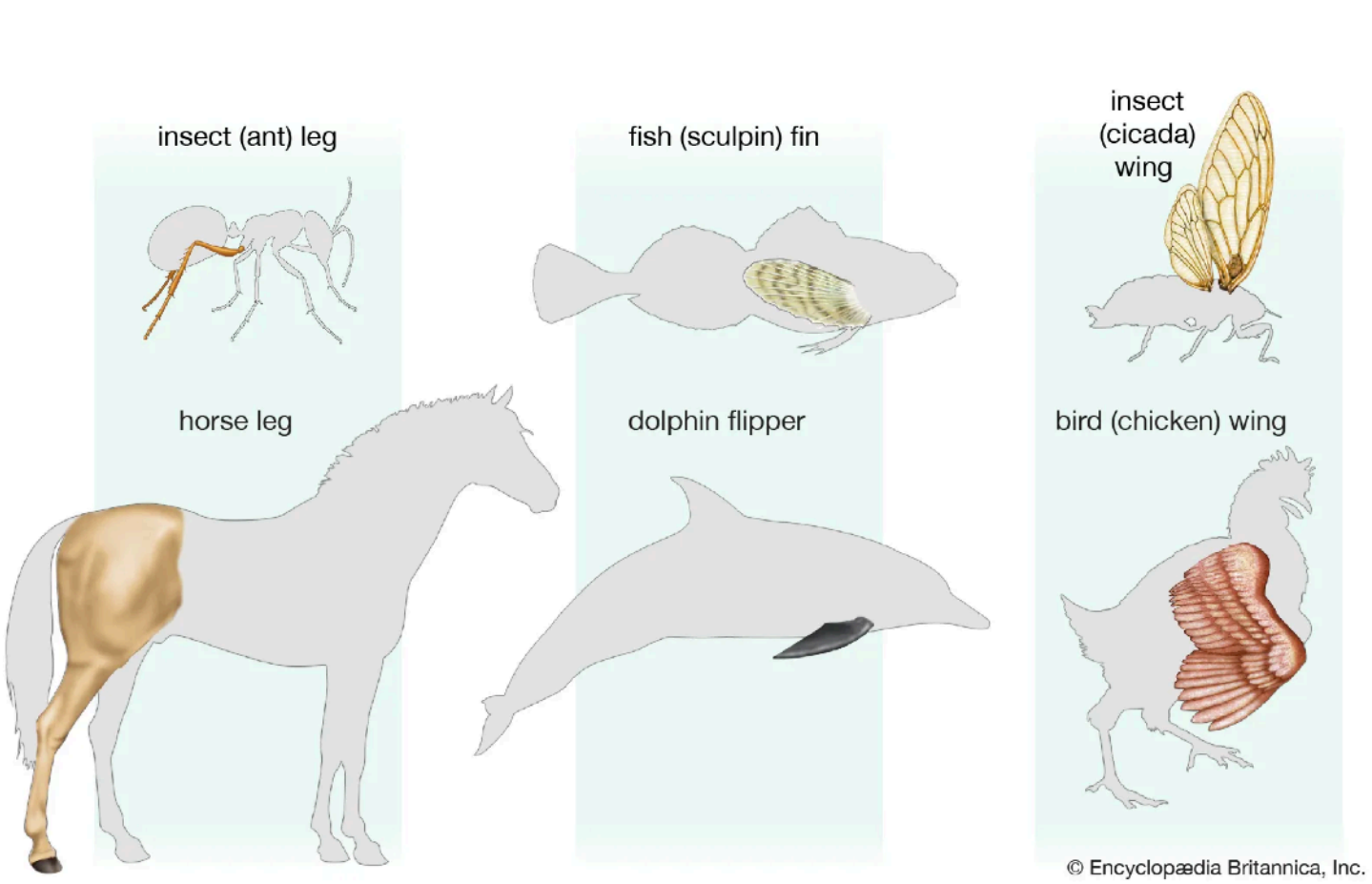
insect (ant) leg
fish (sculpin) fin
insect (cicada) wing
horse leg
dolphin flipper
bird (chicken) wing
© Encyclopædia Britannica, Inc.

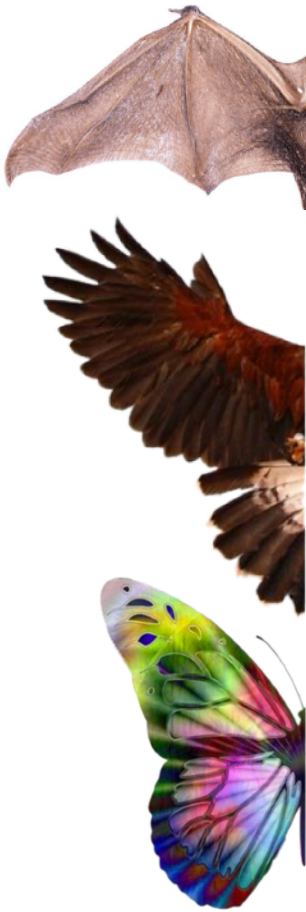

Root

Stem

Developmental homology

Gill slits
Gill slits
Tail
Tail
Fish
Reptile
Bird
Human

Early (tailbud embryo)
Intermediate (late embryo/ early larva)
Late (Adult form visible)
lamprey Petromyzon marinus
dogfish Squalus acanthias
gar Lepisosteus osseus
salmon Salmo salar
lungfish Neoceratodus forsteri
axolotl Ambystoma mexicanum
hellbender Cryptobranchus alleghenensis
snake Natrix natrix
chicken Gallus gallus
possum Trichosurus vulpecula
cat Felis catus
bat Rhynchonycteris naso
human Homo sapiens

Molecular homology

Genetic material

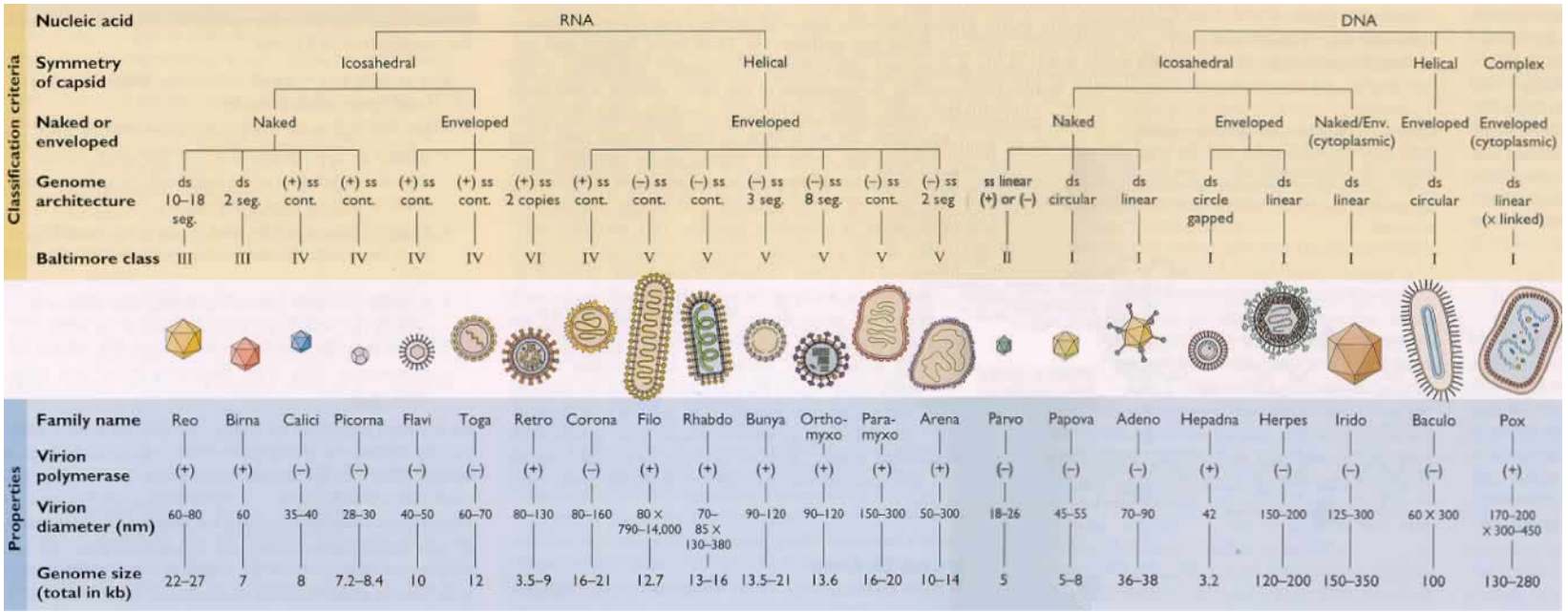
Classification criteria
Nucleic acid
RNA
DNA
Symmetry of capsid
Icosahedral
Helical
Icosahedral
Helical
Complex
Naked or enveloped
Naked
Enveloped
Enveloped
Naked
Enveloped
Naked/Env. (cytoplasmic)
Enveloped
Enveloped (cytoplasmic)
Genome architecture
ds 10–18 seg.
ds 2 seg.
(+) ss cont.
(+) ss cont.
(+) ss cont.
(+) ss cont.
(+) ss 2 copies
(+) ss cont.
(–) ss cont.
(–) ss cont.
(–) ss 3 seg.
(–) ss 8 seg.
(–) ss cont.
(–) ss 2 seg
ss linear (+) or (–)
ds circular
ds linear
ds circle gapped
ds linear
ds linear
ds circular
ds linear (× linked)
Baltimore class
III
III
IV
IV
IV
IV
VI
IV
V
V
V
V
V
V
II
I
I
I
I
I
I
I
Properties
Family name
Reo
Birna
Calici
Picorna
Flavi
Toga
Retro
Corona
Filo
Rhabdo
Bunya
Ortho-myxo
Para-myxo
Arena
Parvo
Papova
Adeno
Hepadna
Herpes
Irido
Baculo
Pox
Virion polymerase
(+)
(+)
(–)
(–)
(–)
(–)
(+)
(–)
(+)
(+)
(+)
(+)
(+)
(+)
(–)
(–)
(–)
(+)
(–)
(–)
(–)
(+)
Virion diameter (nm)
60–80
60
35–40
28–30
40–50
60–70
80–130
80–160
80 × 790–14,000
70–85 × 130–380
90–120
90–120
150–300
50–300
18–26
45–55
70–90
42
150–200
125–300
60 × 300
170–200 × 300–450
Genome size (total in kb)
22–27
7
8
7.2–8.4
10
12
3.5–9
16–21
12.7
13–16
13.5–21
13.6
16–20
10–14
5
5–8
36–38
3.2
120–200
150–350
100
130–280

Molecular homology

Genome organization

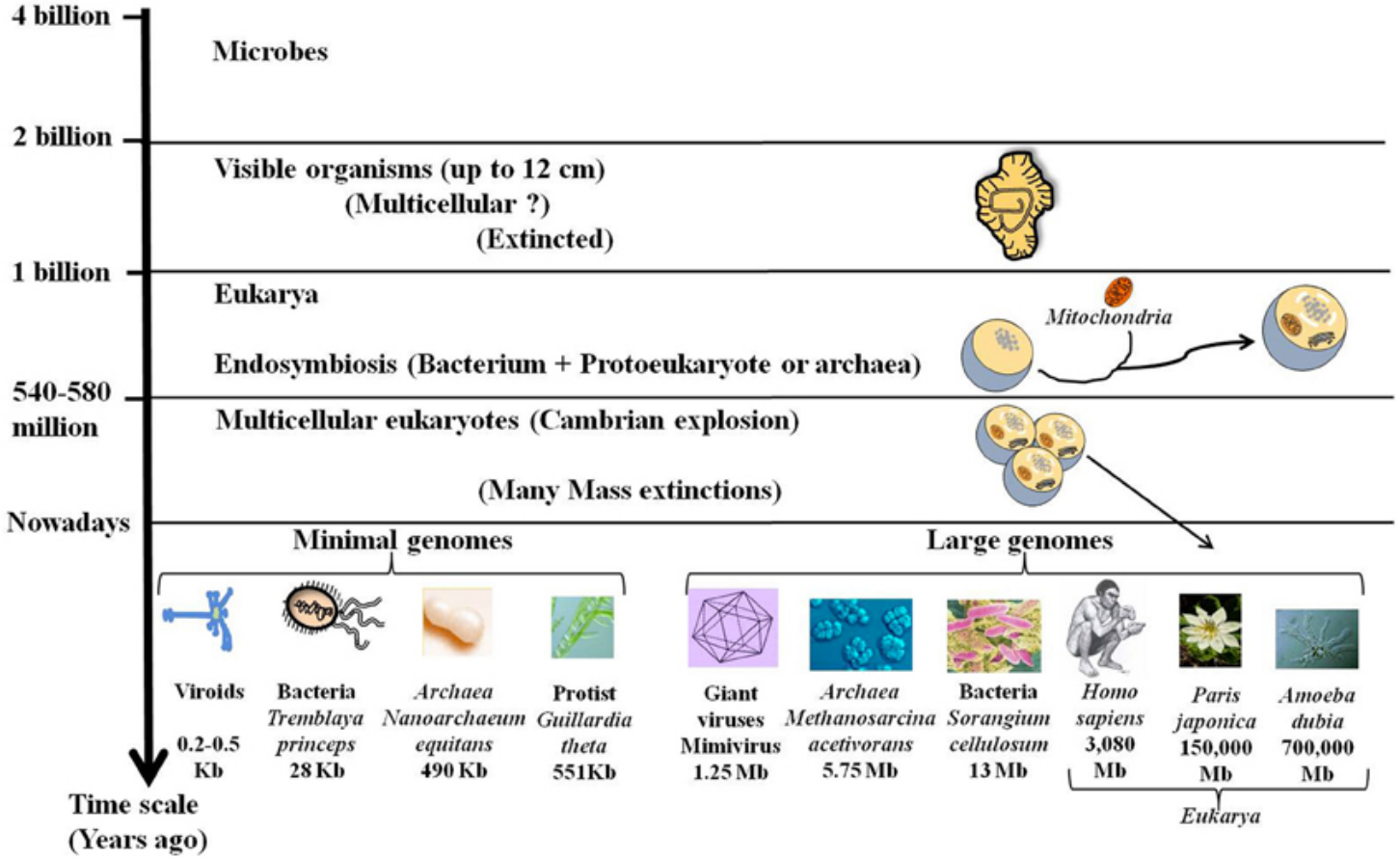
4 billion
Microbes
2 billion
Visible organisms (up to 12 cm)
(Multicellular ?)
(Extincted)
1 billion
Eukarya
Endosymbiosis (Bacterium + Protoeukaryote or archaea)
Mitochondria
540-580 million
Multicellular eukaryotes (Cambrian explosion)
(Many Mass extinctions)
Nowadays
Minimal genomes
Large genomes
Viroids 0.2-0.5 Kb
Bacteria Tremblaya princeps 28 Kb
Archaea Nanoarchaeum equitans 490 Kb
Protist Guillardia theta 551Kb
Giant viruses Mimivirus 1.25 Mb
Archaea Methanosarcina acetivorans 5.75 Mb
Bacteria Sorangium cellulosum 13 Mb
Homo sapiens 3,080 Mb
Paris japonica 150,000 Mb
Amoeba dubia 700,000 Mb
Eukarya
Time scale
(Years ago)

Molecular homology

Genome size

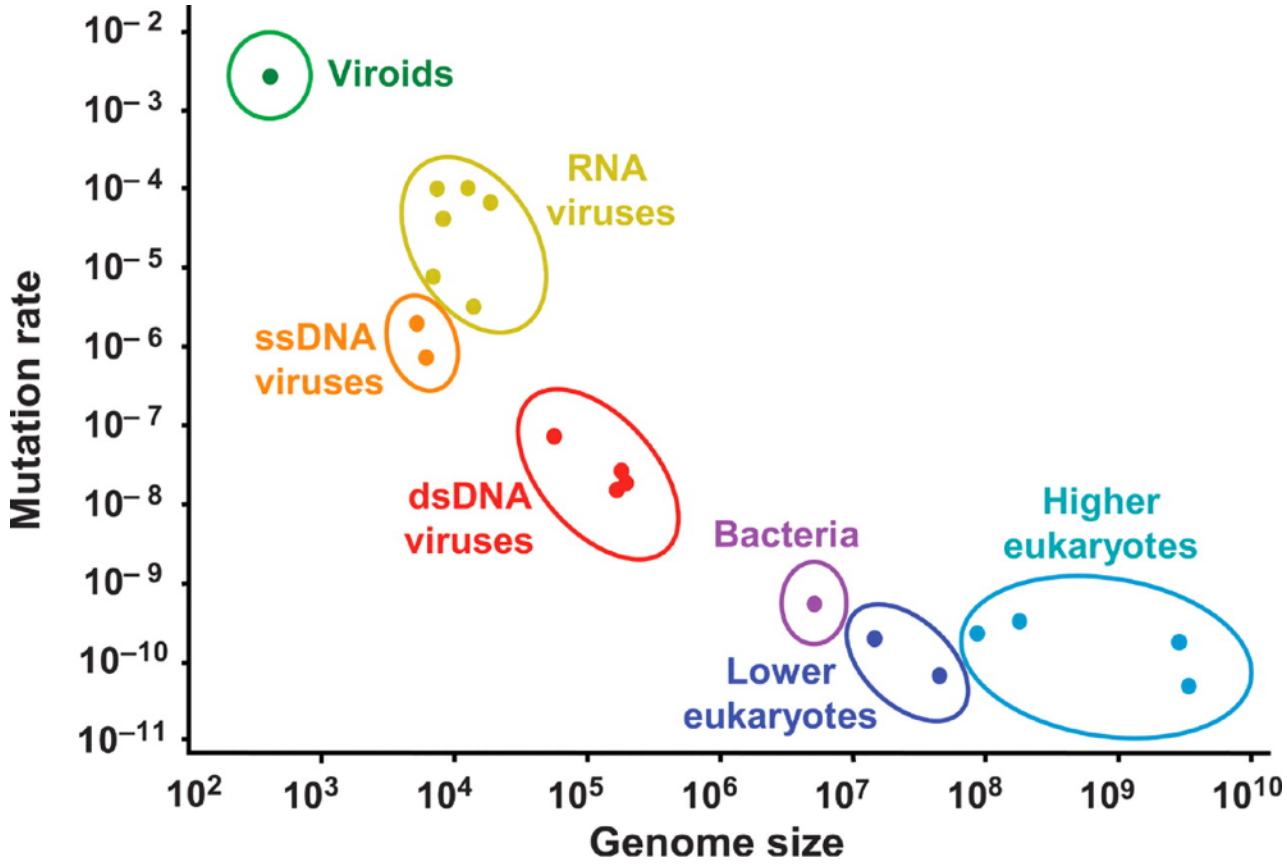

Gago S et. al., (2009). Extremely high mutation rate of a hammerhead viroid. Science 323 (5919):1308

Molecular homology

Gene number

Molecular - Gene number

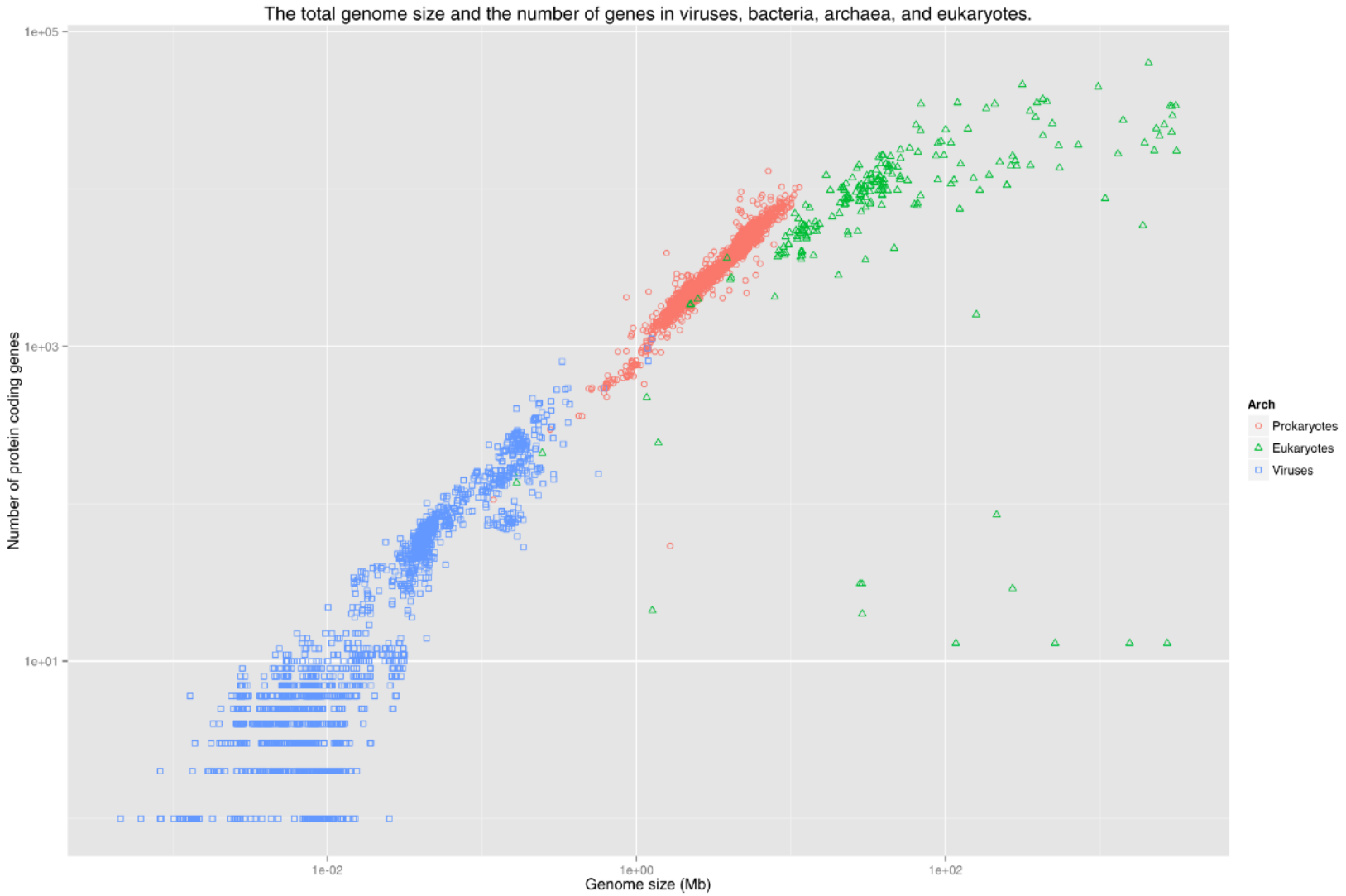

Molecular homology

Synteny

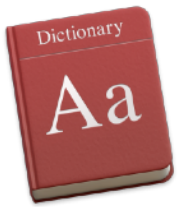

syn·ten·ic | sin'tenik |

adjective

(of genes) occurring on the same chromosome: *syntenic sequences*.

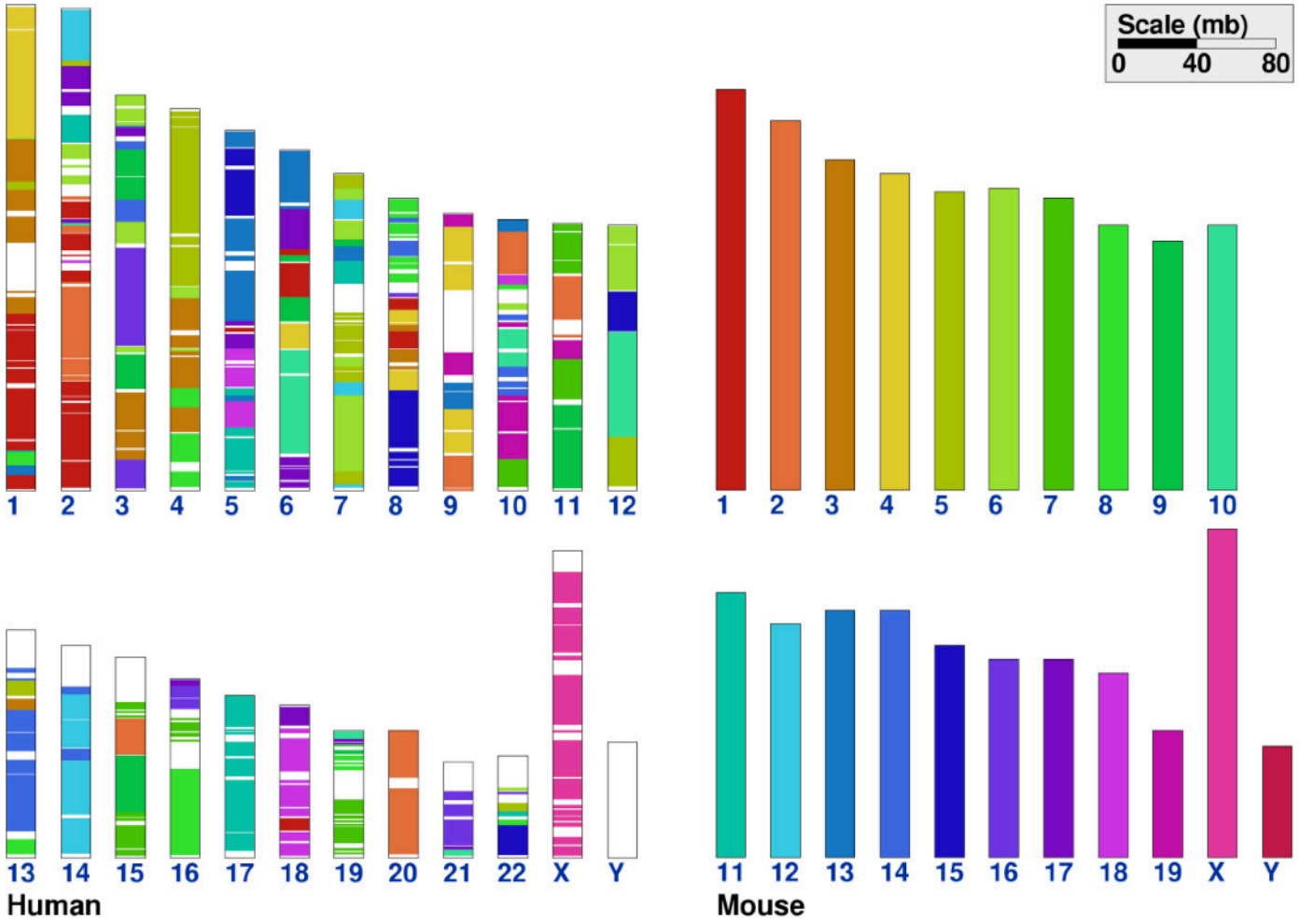
Scale (mb)
0 40 80
1 2 3 4 5 6 7 8 9 10 11 12
13 14 15 16 17 18 19 20 21 22 X Y
Human
1 2 3 4 5 6 7 8 9 10
11 12 13 14 15 16 17 18 19 X Y
Mouse

Network-based microsynteny analysis identifies major differences and genomic outliers in mammalian and angiosperm genomes

Tao Zhao[a] and M. Eric Schranz[a,1]

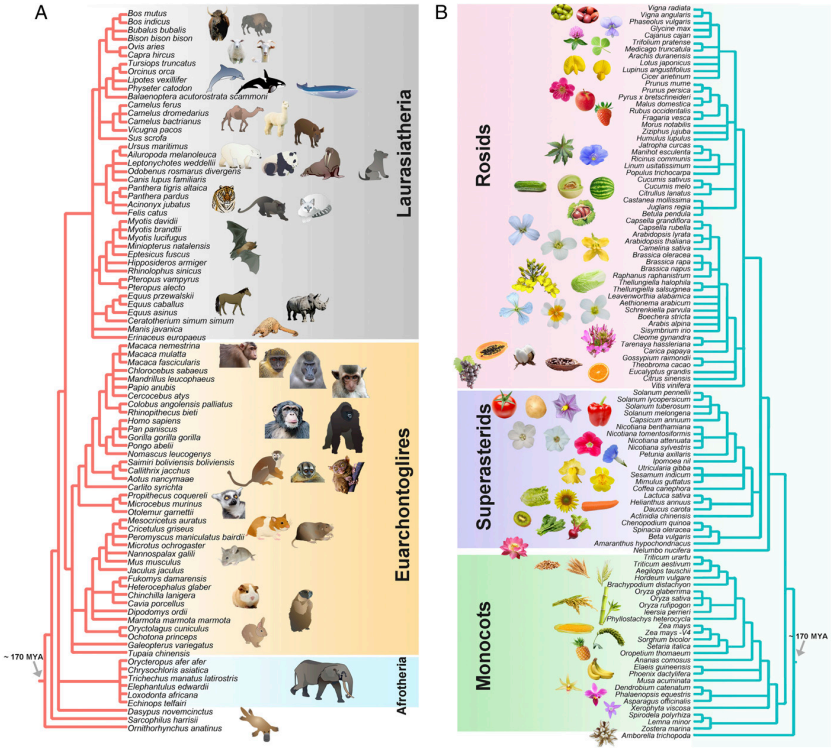

Fig. 2. Phylogenetic relationships of mammalian and angiosperm genomes analyzed. (*A*) Mammal genomes used (tree in red), highlighting the three main placental clades of Laurasiatherias (light-gray shading), Euarchontoglires (light-orange shading), and Afrotheria (light-blue shading). (*B*) Angiosperm genomes used (tree in blue), highlighting the three main clades of rosids (light-red shading), superasterids (light-purple shading), and monocots (light-green shading). The tree and clade shading is maintained in the latter figures. Mammal images courtesy of Tracey Saxby, Diana Kleine, Kim Kraeer, Lucy Van Essen-Fishman, Kate Moore, and Dieter Tracey, Integration and Application Network, University of Maryland Center for Environmental Science (ian.umces.edu/imagelibrary/).

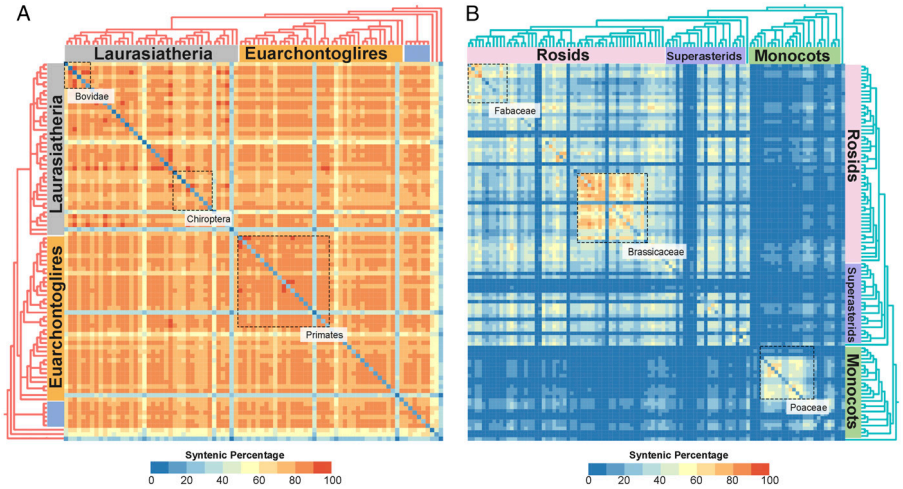

Fig. 3. Pairwise collinearity/microsynteny comparisons of mammalian and angiosperm genomes. (*A*) Pairwise microsynteny comparisons across mammal genomes. (*B*) Pairwise microsynteny comparisons across angiosperm genomes. The color scale indicates the syntenic percentage. Species are arranged according to the consensus phylogeny (Fig. 2). Overall, average microsynteny is much higher across mammals than plants. Also, the detected syntenic percentage does not show a strong phylogenetic signal. For example, contrasts are not higher for intra-Chiroptera (bats) or intra-Bovidae (cattle) than for distant pairwise contrasts. However, it is slightly higher for intraprimate contrasts, whereas, there is a much stronger phylogenetic signal seen for plant genomes such as intra-Brassicaceae or intra-Poaceae (grasses) contrasts than for interfamilial contrasts. The method also allows for easy detection of low-quality genomes. The diagonal for both plots represents intragenome comparisons which can detect potential recent and ancient WGDs. Note, that almost all plant genomes have higher intragenome microsyntenic pair scores than all mammal intragenome comparisons.

PNAS RESEARCH ARTICLE | EVOLUTION OPEN ACCESS

Evolution of the ancestral mammalian karyotype and syntenic regions

Joana Damas[a], Marco Corbo[a], Jaebum Kim[b], Jason Turner-Maier[c], Marta Farré[d], Denis M. Larkin[e], Oliver A. Ryder[f,g], Cynthia Steiner[h], Marlys L. Houck[i], Shaune Hall[i], Lily Shiue[i], Stephen Thomas[i], Thomas Swale[i], Mark Daly[i], Jonas Korlach[k], Marcela Uliano-Silva[l,m,n], Camila J. Mazzoni[m,n], Bruce W. Birren[c], Diane P. Genereux[c], Jeremy Johnson[c], Kerstin Lindblad-Toh[c,o], Elinor K. Karlsson[c,p,q], Martin T. Nweeia[r,s,t], Rebecca N. Johnson[u,v], Zoonomia Consortium[1], and Harris A. Lewin[a,w,x,2]

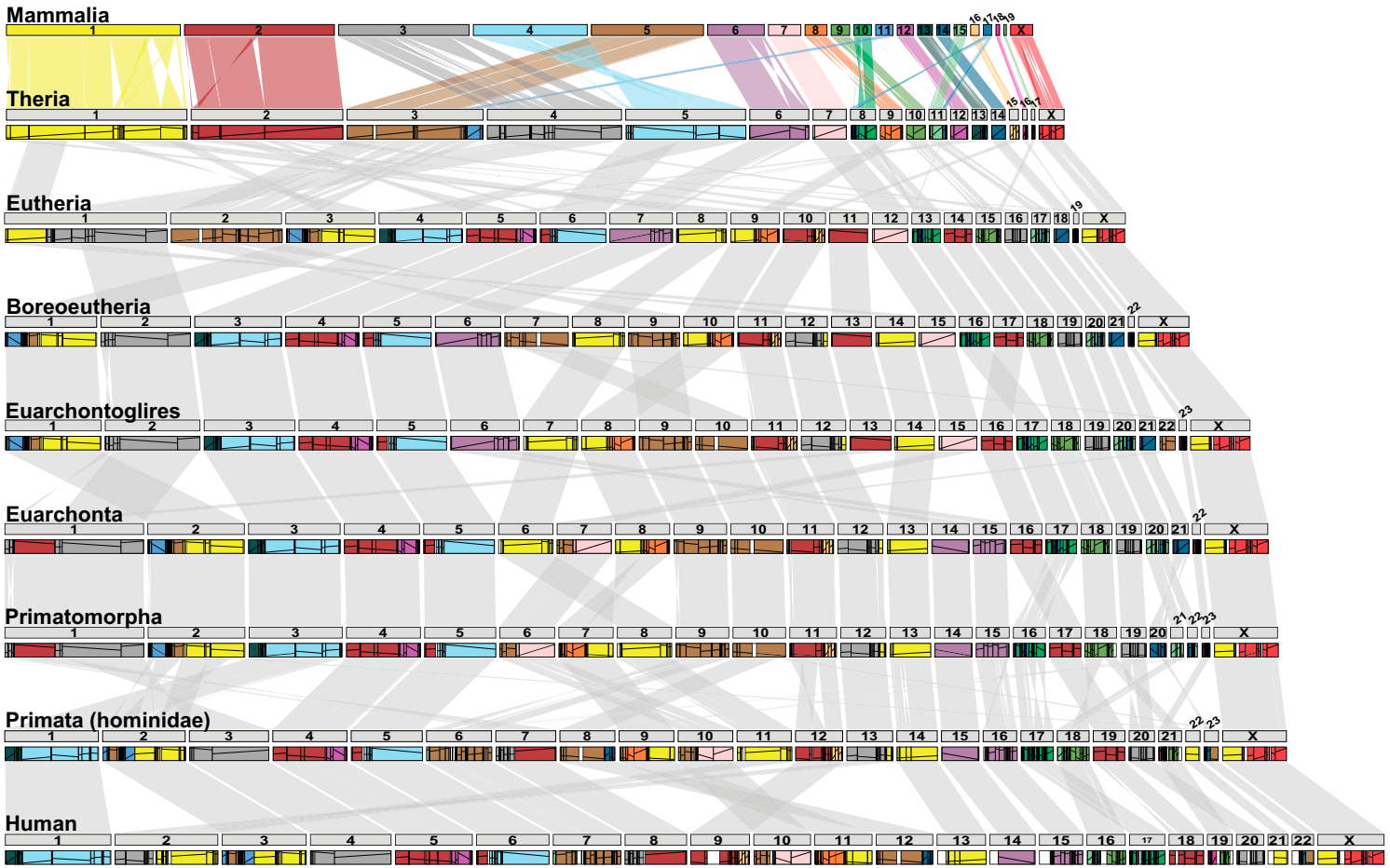

Fig. 2. Evolution of MAMs in the lineage leading to humans. MAMs are distinguished by the colors at the top of the diagram. Colored blocks for every other ancestor and human depict the orthology to MAMs. Lines within colored blocks represent block orientation compared with the MAMs, with positive and negative slopes portraying the same or different orientations, respectively. Gray ribbons depict the orthology of each ancestor to its phylogenetically closest ancestors or species. An orthology map for each pairwise comparison is presented in Dataset S12.

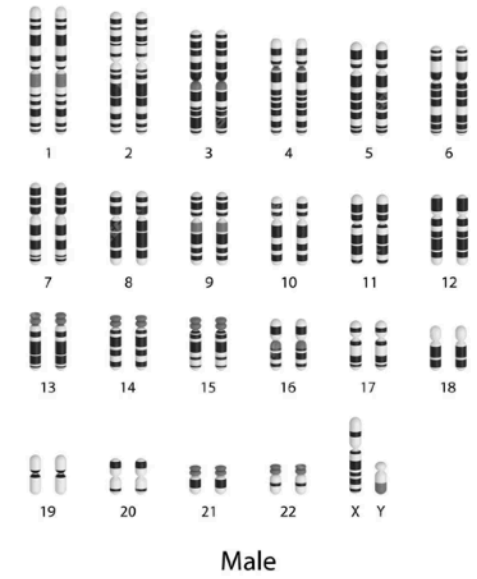

Male

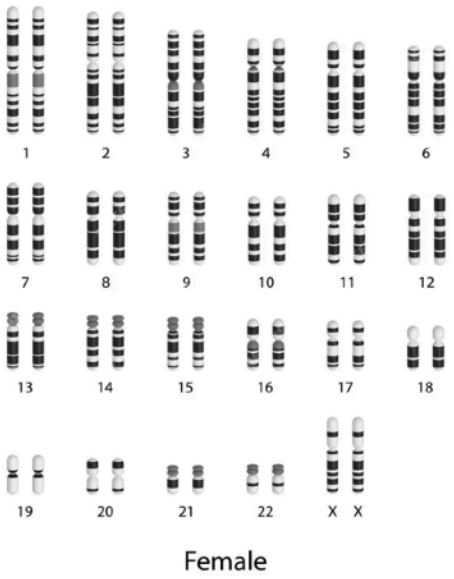

Female

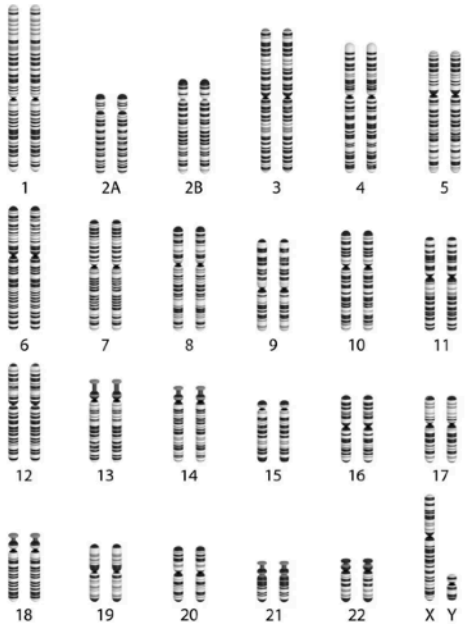

Male

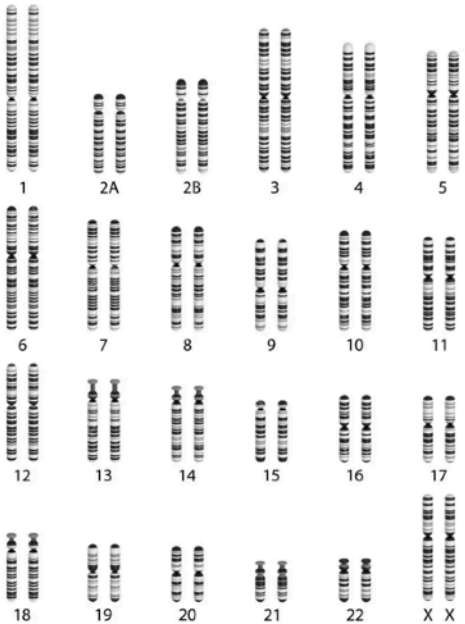

Female

Chromosome 2 (primates)

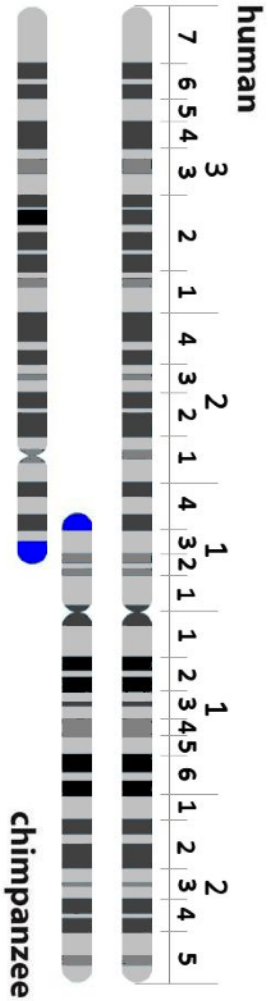

OPEN ACCESS Freely available online

Primer

How and Why Chromosome Inversions Evolve

Mark Kirkpatrick*

Section of Integrative Biology, University of Texas, Austin, Texas, United States of America

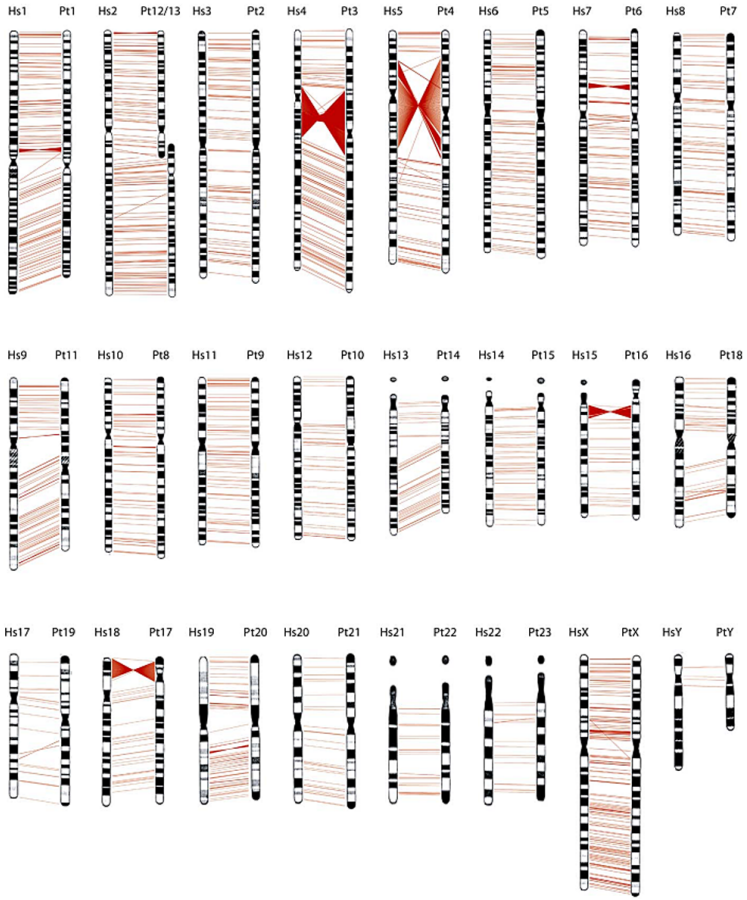

Figure 1. Chromosome inversions that distinguish humans and chimpanzees inferred from a comparison of their genomic sequences [3]. The human chromosome is shown on the left and its chimpanzee homologue on the right for the autosomes and the two sex chromosomes (X and Y). Each red line corresponds to an inversion, with larger inversions (>100 kb) represented by multiple lines.
doi:10.1371/journal.pbio.1000501.g001

Centromere Destiny in Dicentric Chromosomes: New Insights from the Evolution of Human Chromosome 2 Ancestral Centromeric Region

Giorgia Chiatante,[1,2] Giuliana Giannuzzi,[3] Francesco Maria Calabrese,[1] Evan E. Eichler,[4,5] and Mario Ventura*,[1]

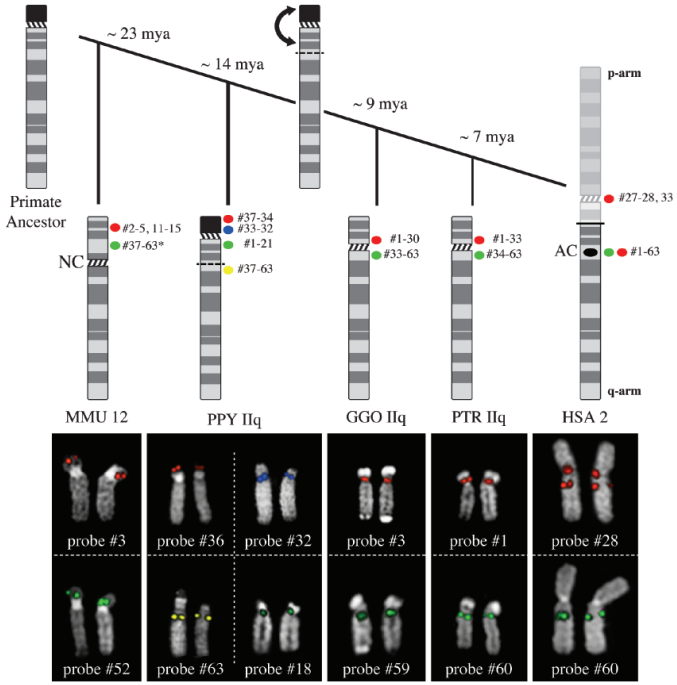

Fig. 2. For every species, probes with the same FISH pattern were grouped and representative results for each class are displayed. In HSA, all fosmids mapped to chromosome 2, only three of them mapped both on the ancestral centromere (AC) and on the primary constriction of chromosome 2 (HSA red signals). For the other species, we used the chromosome IIq active centromere as a landmark. In PTR and GGO, we were able to group the FISH results into two classes, since some probes mapped to the p-side of the centromere, whereas others to the q-side. In PPY, we distinguished four clusters of signals, two for each chromosome arm: we observed distal and proximal signals on both the p- and q-arm. Finally, in MMU we detected signals only on the p-arm, where the inactivated centromere is located. The active centromere is a neocentromere (NC). The * indicates that not all probes from #37 to #63 actually mapped on MMU 12.

Molecular homology

Homeotic genes

Heredity (2006) 97, 235–243

www.nature.com/hdy

SHORT REVIEW

Building divergent body plans with similar genetic pathways

BJ Swalla[1,2,3]
[1]*Center for Developmental Biology, Department of Biology, University of Washington, Seattle, WA 98195-1800, USA;* [2]*Friday Harbor Laboratories, University of Washington, Friday Harbor, WA 98250-9299, USA;* [3]*Smithsonian Marine Station, 701 Seaway Drive, Fort Pierce, FL 34949-3140, USA*

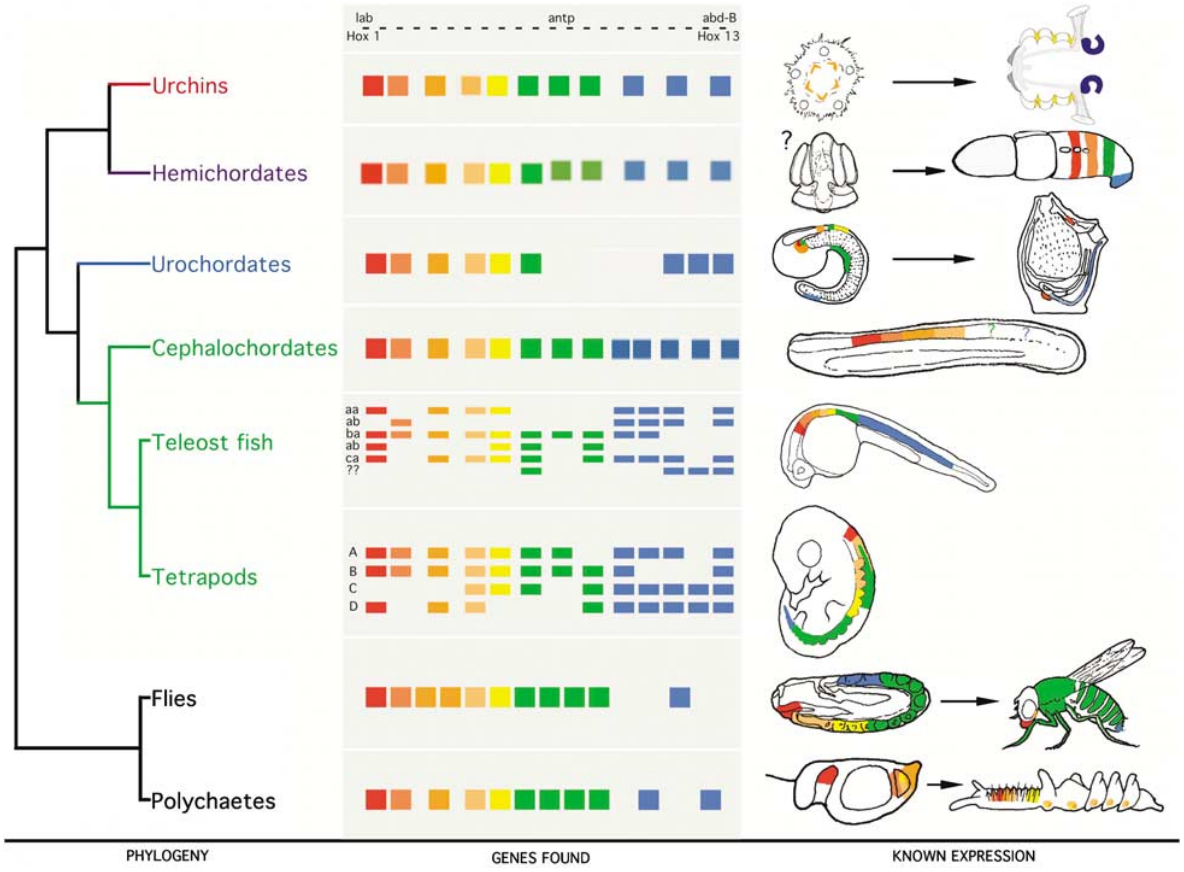

Figure 6 Expression of *Hox* genes in deuterostomes – the *Hox* gene cluster is duplicated in vertebrates. There are eight *Hox* gene clusters in teleost fishes, showing an additional duplication from the four *Hox* gene clusters found in the tetrapod vertebrates. In contrast, the invertebrate deuterostomes each have a single cluster. Ascidians lack some of the middle *Hox* genes, and the cluster is broken up onto two chromosomes. Echinoderms and hemichordates share an independent duplication of the posterior genes, called *Hox 11/13a*, *Hox 11/13b* and *Hox 11/13c*. Hemichordates show anterior to posterior expression in the ectoderm, which will produce a nerve net later in development. Echinoderms show adult expression in the nerve ring with the oral side corresponding to anterior in chordates and hemichordates.

ARTICLE
DOI: 10.1038/s41467-018-04184-x OPEN

Hox and Wnt pattern the primary body axis of an anthozoan cnidarian before gastrulation

Timothy Q. DuBuc[1], Thomas B. Stephenson[2], Amber Q. Rock[2] & Mark Q. Martindale[2]

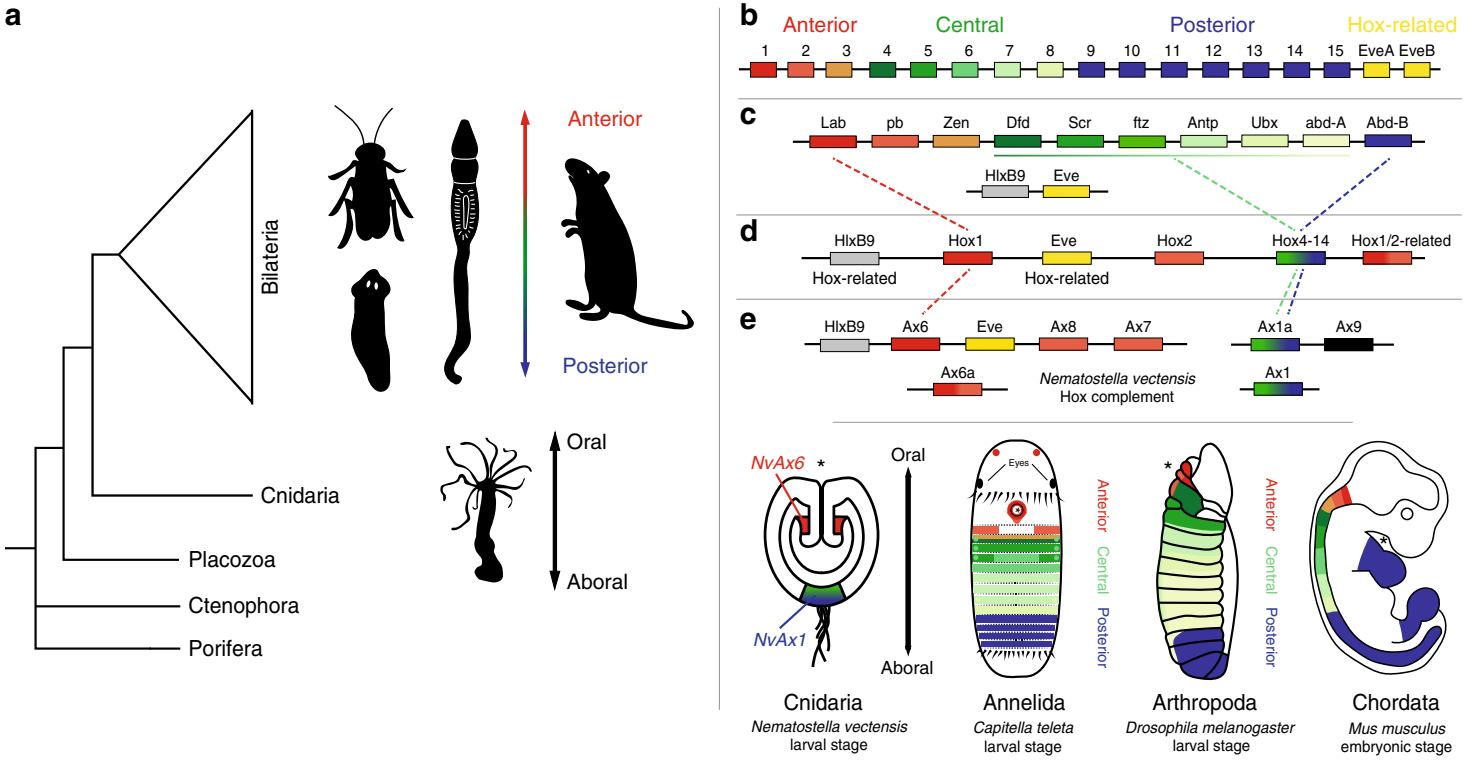

Fig. 1 Anterior–posterior patterning and the emergence of a *Hox* cluster. **a** Bilaterians are classically defined by an anterior–posterior axis perpendicular to the dorsal ventral axis. Cnidarians are the sister taxa to bilaterians and are the only basal lineage to have a diverse cluster of *Hox* genes. **b** The common ancestor of the deuterostome lineage likely had a *Hox* cluster consisting of 14–15 *Hox* genes, closely associated with the homeobox gene *Eve*[18]. **c** Evidence from the protostome, *Tribolium castaneum*, suggests that the protostome ancestor also had an intact *Hox* cluster consisting of at least 10 linked *Hox* genes[17,70]. **d** The cnidarian ancestor had both anterior (*Hox*1 and *Hox*2) and central/posterior (*Hox*9–13) class *Hox* genes[22]. **e** The *Hox* complement of the anthozoan cnidarian, *Nematostella vectensis*, has phylogenetically anterior (*NvAx6*, *NvAx6a*, *NvAx7*, and *NvAx8*) and central/posterior (*NvAx1* and *NvAx1a*) *Hox* genes[14,15]. Depiction of *Hox* expression along the oral–aboral axis of a cnidarian, and the anterior–posterior axis of invertebrates and vertebrates. The anterior (*NvAx6*) and central/posterior (*NvAx1*) *Hox* genes of *Nematostella* are expressed along the oral–aboral axis during larval development. Regions of anterior, central, and posterior *Hox* expression are designated with shades of red, green, and blue, respectively. Asterisk indicates site of mouth formation

plants

Review

Floral Homeotic Factors: A Question of Specificity

Kevin Goslin, Andrea Finocchio and Frank Wellmer *

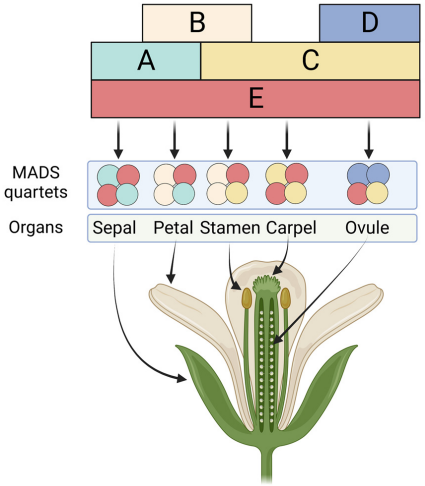

Figure 1. The ABCDE model of floral organ identity specification. The identity of the different floral organs is specified by the combinatorial activity of A-, B-, C-, D-, and E-class genes (as indicated). The MADS-domain transcription factors encoded by these genes act together in different tetrameric complexes ('quartets') to control the developmental programs needed for the formation of sepals, petals, stamens, carpels, and ovules. Colors indicate the composition of the different MADS-domain protein quartets. Figure created with BioRender.com.

Primer

The ABC model of floral development

Vivian Irish

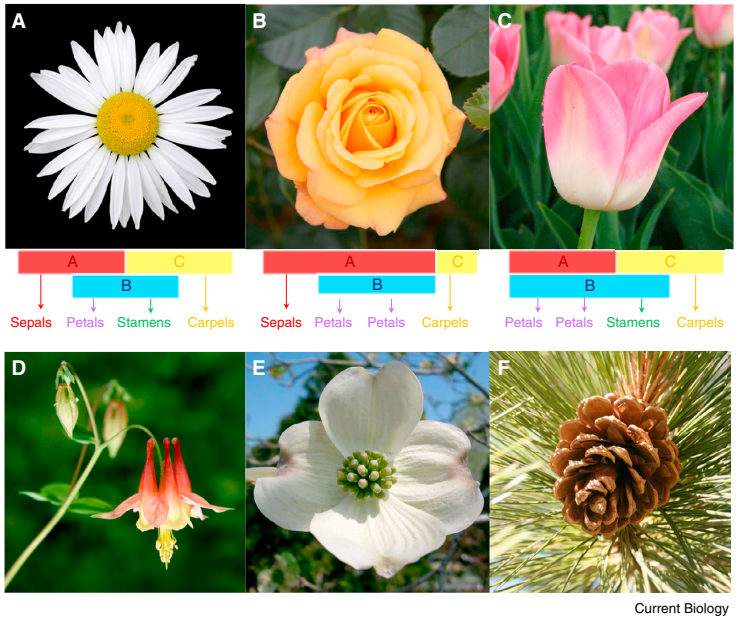

Figure 3. Variations on the ABC theme.
(A) Ox-eye Daisy (*Leucanthemum vulgare)* showing the marginal ray flowers and the central disc flowers; despite the different morphologies of each flower type, the organization of each can be explained by the ABC model (illustrated below). (B) Rose (*Rosa* spp.) with multiple whorls of petals that correspond to an expansion of A + B gene activities (below). (C) Tulip (*Tulipa gesneriana*) with sepal-like organs in the first and second whorls; this can be explained by a shift in the domain of B gene function (below). (D) Columbine (*Aquilegia formosa*) flowers contain stamenodia, a novel organ type situated between the stamens and the carpels. (E) Flowering dogwood (*Cornus florida*) possesses small greenish flowers surrounded by four large, showy petaloid bracts. (F) A female pine cone (*Pinus strobus*). (All images in Figure 3 from Wikimedia commons.)

Molecular homology

Genetic code

Genetic Codon Chart

	U		C		A		G		
U	UUU	Phe	UCU	Ser	UAU	Tyr	UGU	Cys	U
	UUC	Phe	UCC	Ser	UAC	Tyr	UGC	Cys	C
	UUA	Leu	UCA	Ser	UAA	Stop	UGA	Stop	A
	UUG	Leu	UCG	Ser	UAG	Stop	UGG	Trp	G
C	CUU	Leu	CCU	Pro	CAU	His	CGU	Arg	U
	CUC	Leu	CCC	Pro	CAC	His	CGC	Arg	C
	CUA	Leu	CCA	Pro	CAA	Gln	CGA	Arg	A
	CUG	Leu	CCG	Pro	CAG	Gln	CGG	Arg	G
A	AUU	Ile	ACU	Thr	AAU	Asn	AGU	Ser	U
	AUC	Ile	ACC	Thr	AAC	Asn	AGC	Ser	C
	AUA	Ile	ACA	Thr	AAA	Lys	AGA	Arg	A
	AUG	Met	ACG	Thr	AAG	Lys	AGG	Arg	G
G	GUU	Val	GCU	Ala	GAU	Asp	GGU	Gly	U
	GUC	Val	GCC	Ala	GAC	Asp	GGC	Gly	C
	GUA	Val	GCA	Ala	GAA	Glu	GGA	Gly	A
	GUG	Val	GCG	Ala	GAG	Glu	GGG	Gly	G

Translation START codon

Translation STOP codon

Positively charged amino acids

Negatively charged amino acids

Hydrophobic amnio acids

Hydrophilic non-charged amino acids

Cysteine

Genomics: Evolution of the Genetic Code

Patrick J. Keeling
Canadian Institute for Advanced Research, Botany Department, University of British Columbia, 3529-6270 University Boulevard, Vancouver, BC, V6T 1Z4, Canada
Correspondence: pkeeling@mail.ubc.ca
http://dx.doi.org/10.1016/j.cub.2016.08.005

The genetic code is not *quite* universal. The rare variations that we know of reveal selective pressures on the code and on the translation machinery. New data suggest the code changes through ambiguous intermediates and that termination is context dependent.

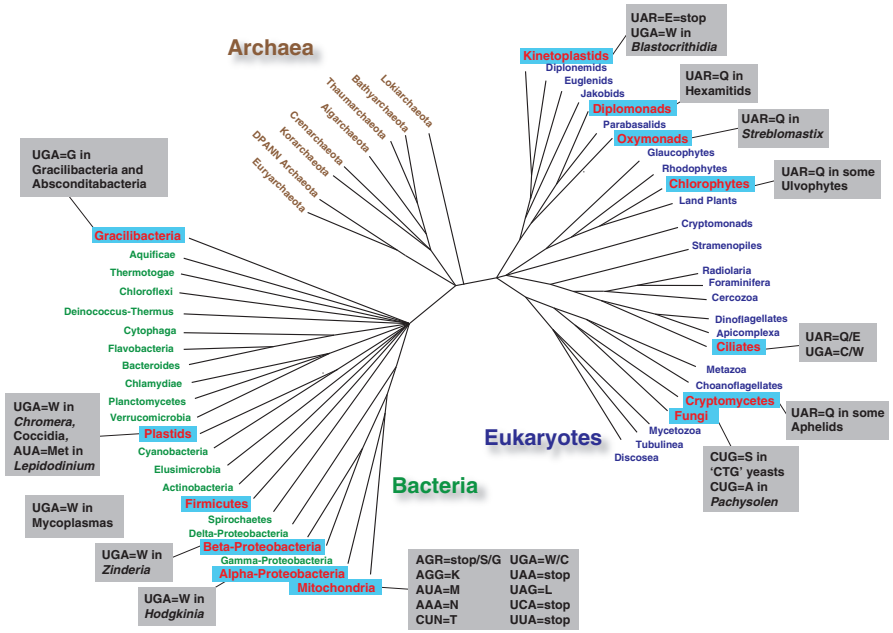

Current Biology

Figure 1. Variation in the genetic code.
Schematic tree of life showing known variations in the genetic code within the three domains of life — Archaea, eukaryotes, and Bacteria (including mitochondria and plastids). Alternative start codons are not included, and are relatively common, and ambiguous codons are listed by their non-canonical codon use only. Of particular note is the strong bias in changes between bacterial (UGA=W) and nuclear genomes (UAR=Q).

Origins of tmRNA: the missing link in the birth of protein synthesis?

Kevin Macé[1] and Reynald Gillet[1,2,*]

[1]Université de Rennes 1, CNRS UMR 6290 IGDR, Translation and Folding Team, 35042 Rennes cedex, France and [2]Institut Universitaire de France

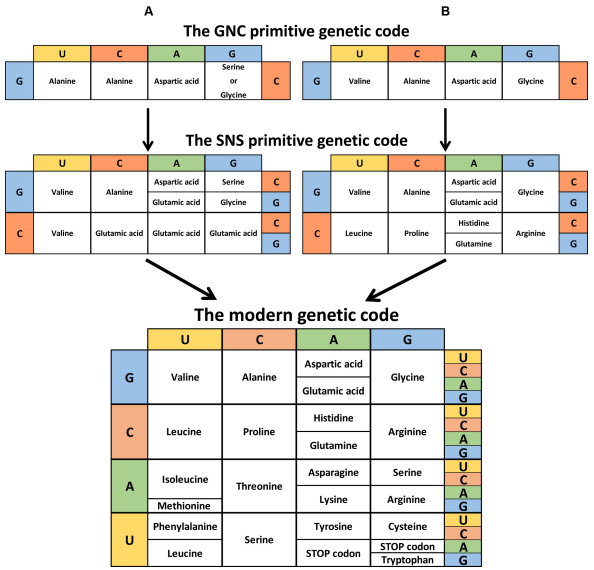

Figure 2. Theory of the genetic code evolution. This shows the evolutionary pathway going from the GNC code (4 codons) to the SNS code (16 codons) to the universal genetic code (64 codons). (**A**) Adapted from Massimo Di Giulio (72). (**B**) Adapted from Kenji Ikehara (10). (**C**) Instead of the conventional representation, the modern genetic code is shown reflecting the order of codon occurrence (columns G and U inverted).

Molecular homology
Psuedogenes

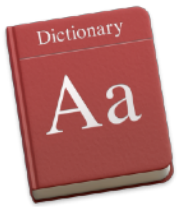

pseu·do·gene | ˈsōōdōˌjēn |

noun *Genetics*

a section of a chromosome that is an imperfect copy of a functional gene.

Overcoming challenges and dogmas to understand the functions of pseudogenes

Seth W. Cheetham, Geoffrey J. Faulkner and Marcel E. Dinger

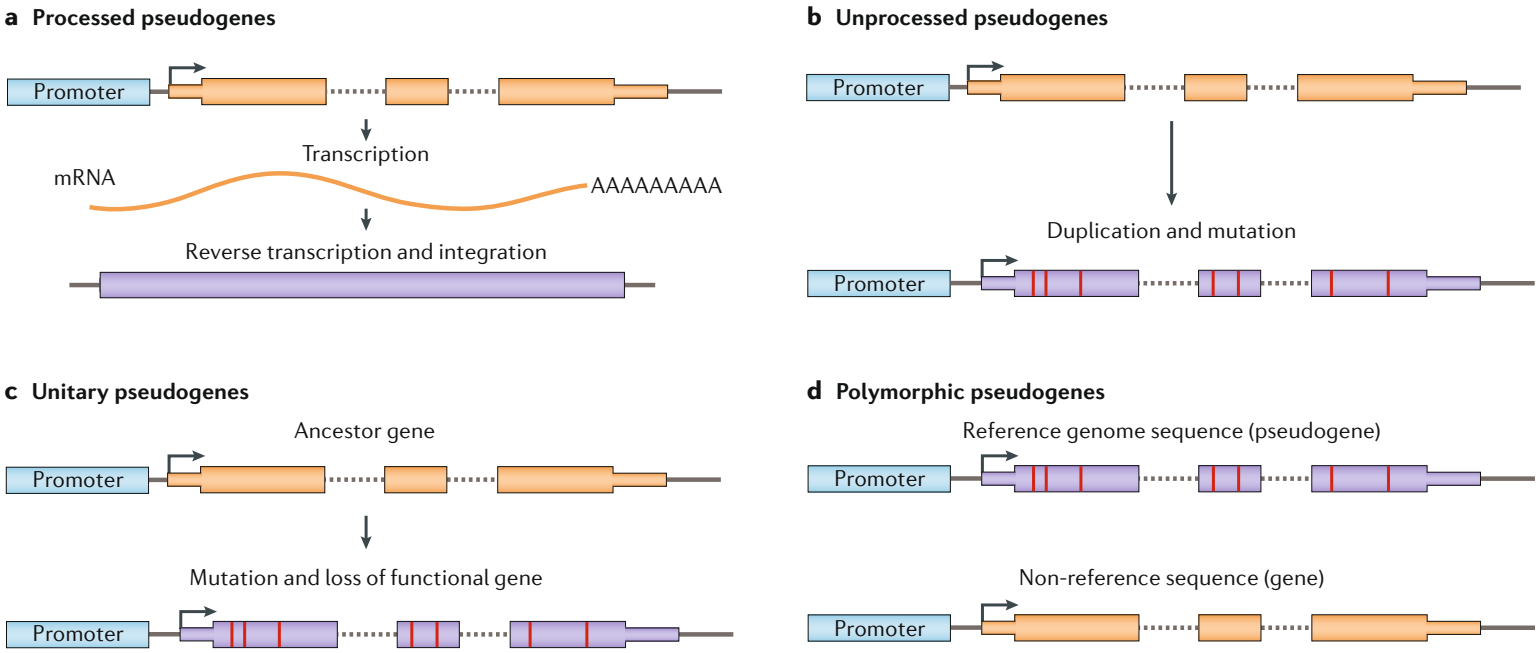

Fig. 1 | **Major classes of eukaryotic pseudogenes. a** | Processed pseudogenes arise from the reverse transcription and integration of a processed mRNA. **b** | Unprocessed pseudogenes originate from gene duplications that accumulate mutations, preventing their translation. **c** | Unitary pseudogenes are derived without duplication from an ancestral protein-coding gene that has lost protein-coding potential. **d** | Polymorphic pseudogenes are sequences that have disabling mutations in the reference genome, but are intact in other non-reference genomes.

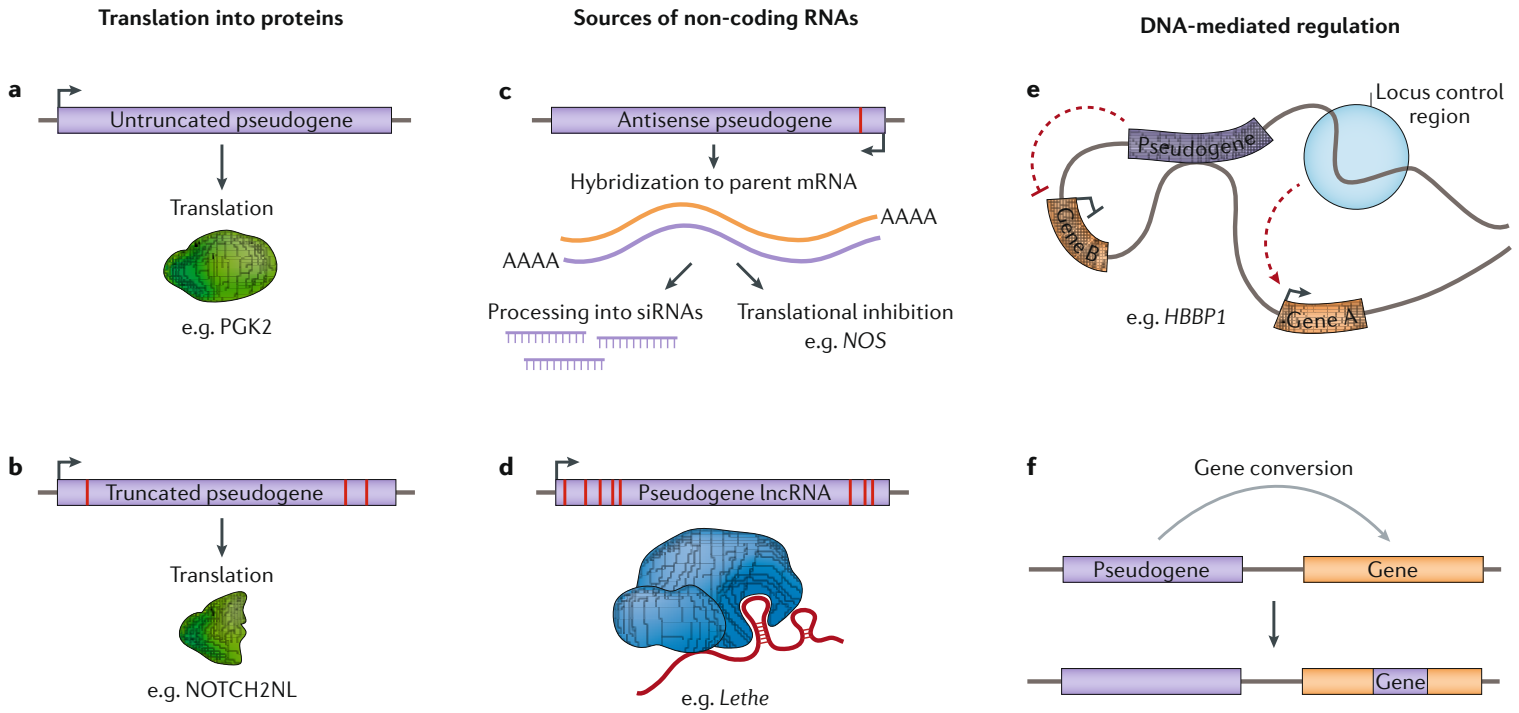

Fig. 2 | **Examples of pseudogene functions. a** | Untruncated pseudogenes can encode full-length proteins with high similarity to their parent genes. **b** | Truncated proteins encoded by pseudogenes can function through intact domains. **c** | Pseudogenes transcribed in antisense relative to their parent genes can form hybrids with parental mRNAs, inhibiting translation. Pseudogene–mRNA hybrids can be processed into small interfering RNAs (siRNAs), inhibiting parental gene expression. **d** | Pseudogenes can encode long non-coding RNAs (lncRNAs) that function through RNA–protein interactions. **e** | Pseudogenes can function in an RNA-independent manner by facilitating 3D chromatin interactions. **f** | Pseudogenes can transfer deleterious alleles to their parental genes by non-allelic recombination (gene conversion).

Molecular homology

Molecular fossils

Identification of an infectious progenitor for the multiple-copy HERV-K human endogenous retroelements

Marie Dewannieux,[1,3] Francis Harper,[2,4] Aurélien Richaud,[1,4] Claire Letzelter,[1] David Ribet,[1] Gérard Pierron,[2] and Thierry Heidmann[1,5]

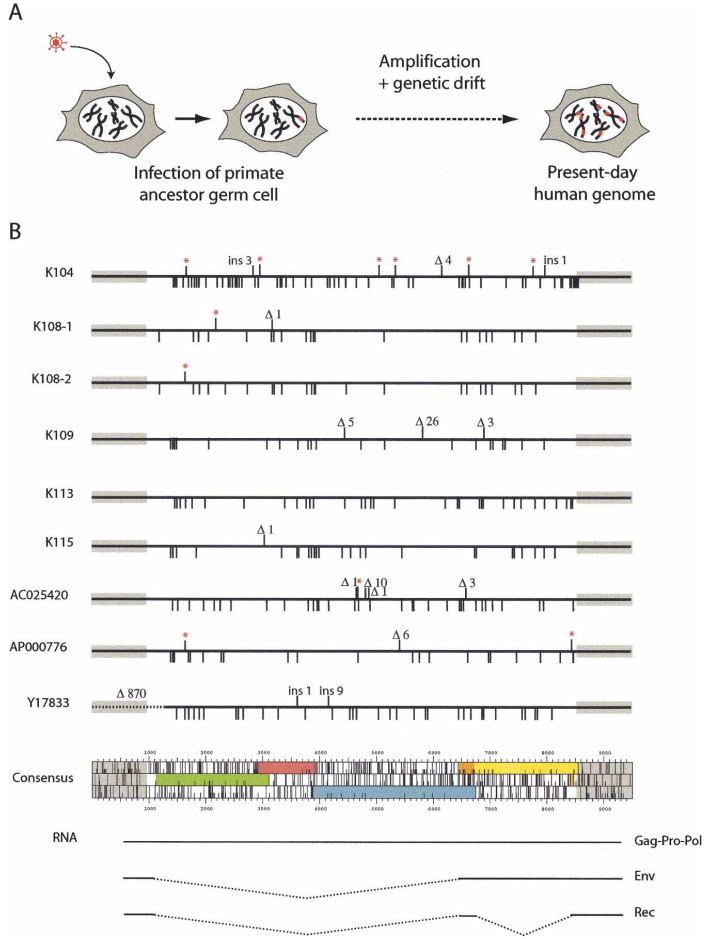

Figure 1. HERV-K(HML2) "endogenization" and present-day human proviruses. (*A*) Evolutionary scheme for HERV-K(HML2) entry into and invasion of the genome of primates. (*B*) Map of the full-length 9.4-kb long human-specific HERV-K(HML2) proviruses and comparison with the in silico-engineered consensus sequence. Each provirus is represented by a solid dark line, with the amino acid substitutions in Gag, Pro, Pol, and Env as compared with the consensus element indicated *below* the line, and the insertions/deletions (ins/Δ) and premature Stop codons (red stars) indicated *above* the line. The ORF map of the consensus provirus is shown, with *gag* in green, *pro* in pink, *pol* in blue, *env* in orange and yellow, the bipartite *rec* in orange, and the two LTRs as gray boxes. (Note that the first coding exon of *rec* belongs to the *env* ORF). The transcripts responsible for the expression of the viral proteins, with the corresponding spliced out domains (dotted lines), are schematized *below* the ORF map.

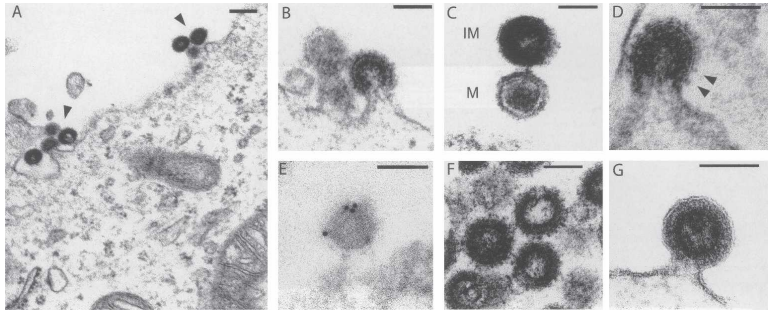

Figure 2. Electron microscopy of the viral-like particles generated by the *Phoenix* provirus. Human 293T cells were transfected with an expression vector for *Phoenix* (*A–E*), or mutants (*F,G*), and observed 48 h post-transfection. (*A*) Low magnification of particles assembled at the cell membrane. (*B*) Representative image of particles budding from the plasma membrane. (*C*) High magnification of two particles, one of which (*bottom*) discloses a mature (M) morphology with a condensed core, while the other appears to be still immature (IM) with two dark peripheral rings surrounding an electron-lucent core. (*D*) High magnification of a particle with prominent spikes, corresponding to the Env protein. (*E*) Image of a particle after labeling with an antibody specific for the HERV-K envelope protein and a secondary antibody linked to gold beads, obtained by immuno-electron microscopy. Quantification of the labeling on 11 independent fields demonstrates association of the gold beads with the viral particles: 307 ± 121 gold beads/μm^2 for the viral particles, versus 4.9 ± 3.2 and 1.1 ± 1.5 gold beads/μm^2 for the cytoplasm and particle-free extracellular space, respectively ($P < 0.001$ between viral particles and any of the two other compartments, Student's *t*-test). (*F*) Image of representative particles obtained after transfection with an expression vector for the *Phoenix pro* mutant. All of them disclosed an immature morphology (41 of 41 identified "free" particles, i.e., no more in the budding process, for the *pro* mutant, vs. 15 of 37 for *Phoenix* WT). (*G*) High magnification of a particle obtained after transfection with an expression vector for the *Phoenix env* mutant. The membrane surrounding the particle is clearly detectable, without any spike. Scale bars: (*A*): 200 nm, (*B–G*):100 nm.

Disclaimer

Figures, photos, and graphs in my lectures are collected using google searches. I do not claim to have personally produced the material (except for some). I do cite only articles or books used. I thank all owners of the visual aid that I use and apologize for not citing each individual item. If anybody finds the inclusion of their material in my lectures a violation of their copy rights, please contact me via email.

hhalhaddad@gmail.com